Electronic Thesis and Dissertation Repository

6-15-2021 9:00 AM

Blocking PirB Function Increases Dendritic Spine Density in the Prefrontal Cortex of Adult Rats

Hannah J. MacNeil, *The University of Western Ontario*

Supervisor: Rajakumar, Nagalingam, *The University of Western Ontario*
Co-Supervisor: Allman, Brian L., *The University of Western Ontario*
A thesis submitted in partial fulfillment of the requirements for the Master of Science degree in Neuroscience
© Hannah J. MacNeil 2021

Follow this and additional works at: https://ir.lib.uwo.ca/etd

Part of the Molecular and Cellular Neuroscience Commons

Abstract

Schizophrenia is a psychotic disorder consisting of positive, negative, and cognitive symptoms. While patients currently have access to treatments for the positive and negative symptoms, no satisfactory treatment exists to alleviate the cognitive deficits, which cause severe impairments to the quality of life of patients and their families. Although the mechanisms underlying the cognitive deficits of schizophrenia are not clear, a decreased dendritic spine density on layer 3 pyramidal neurons in the dorsolateral prefrontal cortex has been strongly implicated. Generally, the adult brain is not permissive to the formation of new dendritic spines. Recently, an immune receptor called paired immunoglobulin-like receptor B (PirB) has been identified to play an active role in inhibiting dendritic spine growth in the adult brain. The current thesis infused PirB blocker into the prefrontal cortex of a rat model that recapitulates several neuroanatomical changes and behavioral deficits associated with schizophrenia, and then analyzed dendritic spine densities using Golgi-Cox method and immunohistochemical labelling of Neurabin-2. The results showed a significant increase in spine density in Golgi-Cox impregnated neurons, and increased Neurabin-2 labelling following infusions of PirB blocker compared to vehicle infusions. These results provide a promising first step in the development of a novel treatment for the cognitive deficits of schizophrenia.

Keywords

Schizophrenia; Paired Immunoglobulin-like Receptor B; Golgi-Cox Method; Prefrontal Cortex; Immunohistochemistry; Dendritic Spine; Rat Model; Cognitive Flexibility

Summary for Lay Audience

Schizophrenia is a severe psychiatric disorder characterized by positive, negative, and cognitive symptoms. The cognitive symptoms in schizophrenia consist of deficits in working memory, attention and executive function, and can have negative impacts on the everyday lives of people with this disorder. The cognitive symptoms have been shown to be associated with degenerative changes in neuronal dendrites, particularly loss of dendritic spines; microscopic protrusions on the surface that receive excitatory connections to neurons of the cerebral cortex. As the adult brain does not support regeneration of dendritic spines, this poses a significant impediment to restoring lost connections. The current study was conducted with the aim of increasing the number of dendritic spines in the prefrontal cortex of adult rats that show many of the common symptoms seen in schizophrenia. This was achieved by blocking the function of a regulatory protein called PirB, which had recently been shown to inhibit the growth of new dendritic spines in the visual cortex. The current thesis used two staining techniques: the Golgi-Cox method, which allows for the quantification of individual dendritic spines in a small number of randomly labelled cells; and immunohistochemistry, which allows for a broader scale observation of dendritic spines in a larger population of cells. Our findings show for the first time that the number of dendritic spines can be significantly increased in adult rats by infusing a PirB blocker into the prefrontal cortex, the cortical area implicated in the degeneration of schizophrenia. Ultimately, the work in this thesis provides insight into how PirB regulates dendritic spine growth in the prefrontal cortex, and how to reverse the loss of dendritic spines in this brain region. Considering a loss of dendritic spines in the prefrontal cortex mediates certain cognitive deficits of schizophrenia, these current findings provide a possible first step in developing a novel treatment for these cognitive deficits.

Acknowledgments

First and foremost, I would like to thank my supervisors, Dr. Raj Rajakumar and Dr. Brian Allman for their guidance over the past years. Together, they have pushed me to become a better scientist throughout my degree. Dr. Rajakumar helped me develop the histological skills required to pursue this research project, for which I am incredibly grateful. Dr. Allman helped me gain a better understanding of the behavioral tasks related to my project, and challenged me to think critically throughout each step. I am also grateful for the feedback they both gave me in writing this thesis.

I am incredibly grateful for past and present members of my advisory committee, Dr. Katherine Wilmore, Dr. Wataru Inoue, Dr. Shawn Whitehead, and Dr. Jessica Grahn for providing me with constructive feedback throughout my degree. They helped me develop this project into what it is today. I would especially like to thank Dr. Wataru Inoue for reading my thesis and providing me with feedback.

I would like to thank Dr. Krystyna Wieczerzak for teaching me how to perform the cannulae implantation surgery and the drug infusions. This project could not have occurred without her assistance.

I would like to thank Kyla Lee for administering the NGF infusions to produce the animal model used for this study.

I would like to thank Sabeszan Jeganathan for his help with the stress paradigm used in this thesis.

I would like to thank all members of the Allman and Rajakumar labs for their continued support and for helping me develop my presentation skills over the past few years.

Finally, I would like to thank the professors and staff in the Neuroscience Graduate Program for ensuring that my graduate experience was a seamless and enjoyable as it could be.

Table of Contents

List of Figures

List of Appendices

List of Abbreviations

ABP, Actin Binding Protein

Arp2/3, Actin Related Protein 2/3

BCCAO, Bilateral Common Carotid Artery Occlusion

BSA, Bovine Serum Albumin

BZ, Binocular Zone

CA1, Cornu Ammonis 1

CA3, Cornu Ammonis 3

Cg1, Cingulate Cortex

CNS, Central Nervous System

DISC1, Disrupted-in-Schizophrenia-1

dlPFC, Dorsolateral Prefrontal Cortex

ERK, Extracellular Receptor Kinase

F-actin, Filamentous Actin

fMRI, Functional Magnetic Resonance Imaging

GABA, Gamma Aminobutyric Acid

G-actin, Globular Actin

IRSp53, Insulin Receptor Substrate p53

ITIM, Immunoreceptor Tyrosine-base Inhibitory Motif

LILB2, Leukocyte Immunoglobulin-like Receptor B2

LTP, Long Term Potentiation

M1, Primary Motor Cortex

M2, Supplementary Motor Cortex

MAG, Myelin-Associated Glycoprotein

mEPSP, Miniature Excitatory Post-Synaptic Potential

mGluR, Metabotropic Glutamate Receptor

MHC1, Major Histocompatibility Complex Class 1

mPFC, Medial Prefrontal Cortex

NGF, Nerve Growth Factor

NMDA, N-methyl-D-aspartate

NogoA, Neurite Outgrowth Inhibitor A

OCT, Optimal Cutting Temperature compound

OD, Ocular Dominance

PAK, p21-Activated Kinases

PB, Phosphate Buffer

PBS, Phosphate Buffered Saline

PE, PirB Ectodomain

PFC, Prefrontal Cortex

PirB, Paired Immunoglobulin-like Receptor B

PKC, Protein Kinase C

PPAR-γ, Peroxisome Proliferator-Activated Receptor-γ

PSD, Post Synaptic Density

SEM, Standard Error of the Mean

WCST, Wisconsin Cart Sorting Task

Chapter 1

1 Dendritic Spines: Structure, Function & Plasticity

Dendritic spines are small protrusions along the dendrites of neurons that receive most of the excitatory input in the mammalian brain. Changes in dendritic spine structure occur constantly in the healthy brain; however, problems arise when spine densities decrease significantly. Many neurological disorders are associated with the loss of dendritic spines, making them an important target in the development of novel treatments. This chapter summarizes the structure and function of dendritic spines, as well as recent progress toward reversing dendritic spine loss and growing new dendritic spines in the adult brain. Finally, a regulatory immune receptor called Paired Immunoglobulin-like Receptor B (PirB) will be discussed in further detail as it is involved in inhibiting dendritic spine growth, and blocking its activity has shown great promise in reversing dendritic spine loss in multiple brain regions.

1.1 What are dendritic spines?

1.1.1 Morphology

Dendritic spines are small protrusions found along dendrites consisting of a head and a neck, connecting them to the dendritic shaft of a neuron (Reviewed in McGuier et al., 2019). Although dendritic spines vary in size depending on a variety of factors, including the animal species, neuronal type and spine age, they are typically between 0.5-2 µm in length (Reviewed in Sala & Segal, 2014). Dendritic spine densities in mature cortical excitatory neurons typically range from 1-10 spines per 1 µm of dendrite length (Benavides-Piccione et al., 2013). Dendritic spines are found along the dendrites of most projection neurons (i.e., pyramidal neurons of the cerebral cortex that use glutamate, and medium spiny neurons of the striatum that use GABA); however, they are not commonly found on interneurons of the cerebral cortex that release GABA (Reviewed in Hering & Sheng, 2001). Dendrites of mature cerebral cortical pyramidal cells, granule cells of the dentate gyrus, and Purkinje cells in the cerebellum are densely covered with spines (**Fig. 1**). There are four main morphological classes of dendritic spines: mushroom spines,

which contain a large bulbous head; thin spines, which contain a small spine head and a thin, long neck; stubby spines, which do not contain a neck; and filopodia, which are long and thin with no distinguishable spine head (**Fig. 2**).
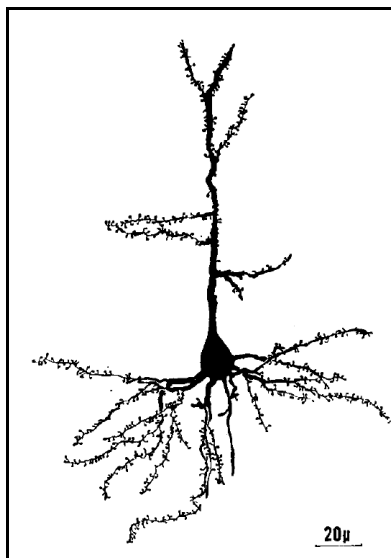
Figure 1. Representative image of a pyramidal cell. Projecting dendrites are densely covered with small protrusions (i.e., dendritic spines) (Adapted from Peters & Kaiserman-Abramof, 1970).
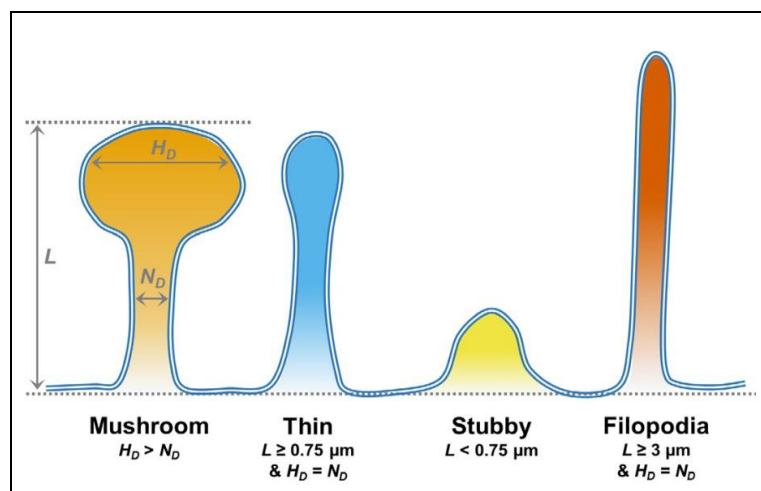
Figure 2. Morphological classification of dendritic spines. The larger, bulbous area is

the spine head, which is attached to the dendrite by the thinner spine neck. L represents spine length, HD represents spine head diameter, and ND represents spine neck diameter (Adapted from McGuier et al., 2019).

Dendritic spines contain an actin-rich cytoskeleton and they vary in structure from simple to complex, with thin spines being the most common type of protrusion found on principal neurons of the central nervous system (CNS). Across the animal kingdom, dendritic spines are typically found in vertebrate brains, such as the mammalian brain, suggesting their important role in the vertebrate CNS (Reviewed in Sala & Segal, 2014). Dendritic spines are dynamic structures that are constantly changing in both structure and size (Reviewed in McGuier et al., 2019). Less than 10% of the spine head is made up of an area called the Postsynaptic Density (PSD), which is directly aligned with the presynaptic active zone to form a synapse (Peters & Kaiserman-Abramof, 1970). The PSD contains many receptors, signaling, and cell-adhesion molecules (Reviewed in Harris, 1999). Larger spines contain more organelles and are typically part of a larger synapse, whereas smaller spines contain less organelles and typically participate in a smaller synapse (Peters & Kaiserman-Abramof, 1970). The dendritic spine is the main input for excitatory information in the mammalian brain, and dendritic spine density directly correlates with the number of excitatory inputs onto a neuron (Reviewed in Harris, 1999).

1.1.2   Development of dendritic spines

The development of dendritic spines is a complex process involving many molecules. The following section summarizes the roles of the main molecules involved in the development of dendritic spines.

Changes in the number of dendritic spines rely heavily on restructuring of the actin cytoskeleton of dendritic spines. Actin filaments are polar structures and restructuring of the actin cytoskeleton occurs by rapid addition to the plus end (i.e., the barbed end) and removal of the minus end (i.e., the pointed end) (see **Fig. 3**). This process is called 'actin treadmilling', and occurs constantly (Blanchoin et al., 2014). The organization of filamentous actin (F-actin) structures determines their lifetime, and varies from a network

of branched filaments, which change very rapidly, to large bundles of multiple cross-linked filaments, which can remain stable for much longer (Blanchoin et al., 2014; Honkura et al., 2008). F-actin organization in dendritic spines varies depending on the part of the spine. For example, F-actin in the spine head is found as a branched network, whereas in the spine neck, both branched and tightly packed linear F-actin are found (Korobova & Svitkina, 2010). This organization suggests that F-actin in the spine head grows and shrinks very rapidly, while the spine neck contains more stable F-actin.
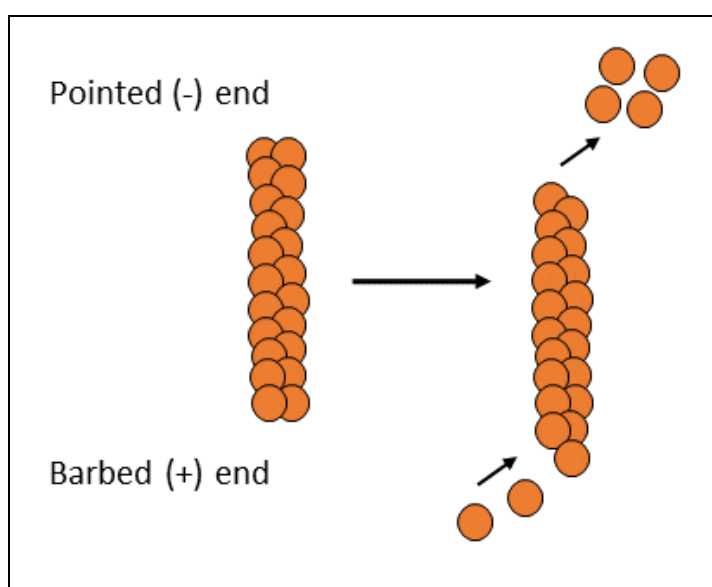
Figure 3. Schematic of actin treadmilling. Actin is rapidly added to the barbed (+) end of the actin filament, while actin is simultaneously being removed from the pointed (-) end of the actin filament.

Actin binding proteins (ABPs) make up a large group of hundreds of proteins that are bound by actin. These ABPs carry out many different functions and are crucial in the development of dendritic spines. Multiple ABPs are responsible for the disassembly of F-actin and can function by capping the pointed and/or barbed ends (e.g., tropomodulin, CapZ), severing the filament by cutting it into two pieces (e.g., gelsolin), or depolymerizing the actin filament and converting it from F- to globular actin (G-actin) (e.g., cofilin, CapZ). Other ABPs assemble the F-actin and function by stabilizing the

filament and preventing depolymerization (e.g., tropomyosin), or by aiding in the formation of actin filament bundles and branching networks (e.g., Arp2/3 complex) (Reviewed in dos Remedios et al., 2003). It is currently thought that dendritic spines originate from dendritic filopodia, which contain both branched and tightly packed F-actin that forms a tip (i.e., the spine head) via activity of the Arp2/3 complex (Kim et al., 2013; Korobova & Svitkina, 2010).

Insulin receptor substrate p53 (IRSp53) is another molecule that has been shown to be involved in the normal development of dendritic spines. IRSp53 is located in the PSD and is involved in regulating F-actin within filopodia (Abbott et al., 1999; Scita et al., 2008), therefore it may play a key role in regulating development of the dendritic filopodia. The mechanism by which IRSp53 functions to regulate F-actin is not fully understood; however, it is thought that in early synaptogenesis, F-actin can bind and deform plasma membranes, generating protrusions in the membrane. In both early and mature synapses, IRSp53 can regulate F-actin branching by polymerizing actin filaments (Reviewed in Kang et al., 2016).

In 2005, Choi and colleagues conducted a study in which IRSp53 was overexpressed in cultured hippocampal neurons. They found that these neurons had an increased dendritic spine density and size, further confirming the role of IRSp53 in spine development. This same study also showed that when IRSp53 was knocked down, the hippocampal cells had a decreased dendritic spine density. Multiple additional studies have been conducted to determine the effects of knocking out IRSp53 in mice and have found that excitatory synapses develop slowly (Sawallisch et al., 2009), and that in the medial prefrontal cortex (mPFC), spine densities and excitatory synapses were decreased (Chung et al., 2015). Additionally, behavioral impairments were observed in IRSp53 knockout mice in tasks such as the Morris water maze, and novel object recognition (Kim et al., 2009), as well as in other behavioral aspects such as 3-chamber social interaction, and ultrasonic vocalization calls to females (Chung et al., 2015). Taken together, these results suggest that proper IRSp53 function is crucial in the normal development of excitatory synapses and dendritic spines in the mPFC and hippocampus.

1.2   Function of dendritic spines

1.2.1   Dendritic spines in the hippocampus

The dynamic nature of dendritic spine structure is associated with activity of the synapse. A series of studies conducted by Fifková and colleagues in the 1970s and 1980s found that long-term potentiation (LTP) could be induced *in vivo* at synapses between hippocampal perforant pathways and dentate granule cells, and that dendritic spines that were located along stimulated pathways were larger than those on unstimulated pathways (Van Harreveld & Fifková, 1975). Additional studies showed that following LTP induction, dendritic spines along stimulated pathways were shorter and wider, thereby providing more efficient transmission at the spine head (Fifková & Anderson, 1981). In the following years, multiple research groups have shown that dendritic spine structure and density undergo many changes following LTP induction (Desmond & Levy, 1986; Engert & Bonhoeffer, 1999; Ostroff et al., 2002). These findings provide strong evidence of the association of dendritic spines and synaptic plasticity in learning and memory. In 2006, Park and colleagues asked: How do spines grow and increase in response to LTP induction? To answer this, they used electron microscopy and live cell imaging to show that LTP induction promotes the mobilization of recycling endosomes and vesicles into spines. Additionally, when recycling endosome transport was blocked, LTP-induced changes in dendritic spines were abolished. Overall, findings of Park et al. (2006) suggest that membrane trafficking from recycled endosomes is required for both the growth and maintenance of dendritic spines in response to LTP.

1.2.2   Dendritic spines in the prefrontal cortex

Apart from the rapid growth of dendritic spines following LTP induction, normal dendritic spine morphology and density are also crucial for tasks involving learning and memory. Furthermore, certain experiences throughout the animal's lifespan can impact the structure and function of dendritic spines in the prefrontal cortex (PFC). For example, repeated stress in young rodents causes a significant decrease in the number of dendritic spines present on layers 2/3 and layer 5 pyramidal cells in the prelimbic area of the PFC (Radley et al., 2006; Yang et al., 2015). Animal models of obesity also show decreased

dendritic spine density, and in turn decreased performance on cognitive tasks (Bocarsly et al., 2015). Aging also causes deficits in dendritic spine growth and maintenance. For example, aged rhesus monkeys have a significantly lower number of excitatory synapses in layers 2/3 of area 46 of the dorsolateral prefrontal cortex (dlPFC) compared to young rhesus monkeys. This decrease in synapse number is directly correlated with a decrease in performance on a delayed nonmatching to sample task (which tests for working memory), as well as a delayed recognition memory span task (Dumitriu et al., 2010; Peters et al., 2008). A study conducted by Bloss and colleagues looked further into the mechanisms of synapse loss as a result of aging and found that aged rodents have a marked reduction in dendritic spine density in the PFC, as well as less experience-dependent plasticity (Bloss et al., 2011).

1.2.3   Dendritic spines in other brain areas

Dendritic spines are involved in receiving excitatory input in many different brain regions, and disruptions to the morphology and/or density of spines exist throughout the brain with differing consequences. For example, in the visual cortex, dendritic spines have been shown to be involved in experience-dependent plasticity, where visually evoked cortical function is inversely related to the dynamic structure of dendritic spines (Tropea et al., 2011). In rhesus monkeys, dendritic spine density in V1 area of the visual cortex decreases with age, similar to what has been described in the PFC of aged animals (Young et al., 2014).

Dendritic spines in the auditory cortex have also been shown to be involved in different types of learning. Moczulska and colleagues used chronic *in vivo* two-photon microscopy to observe dendritic spines in the auditory cortex during auditory-cued classical conditioning in order to test whether the formation of a fear memory correlates with synaptic changes in the mouse auditory cortex. They found that paired conditioning induced an increase in spine formation, while unpaired conditioning induced elimination of spines in the auditory cortex (Moczulska et al., 2013). Another study, conducted by Lai and colleagues in 2018, used transcranial two-photon microscopy to examine changes in dendritic spines on layer 5 pyramidal neurons in the mouse auditory cortex during fear conditioning. These authors found that, similar to classical conditioning, paired fear

conditioning induced spine formation, while unpaired fear conditioning caused the elimination of spines in the mouse auditory cortex (Lai et al., 2018). Taken together, these studies demonstrate the involvement of dendritic spines in the auditory cortex during classical conditioning and during fear conditioning. These results show how important normal spine development and plasticity is for multiple aspects of learning and memory.

1.3 Clinical conditions associated with dendritic spine loss

Many neurological disorders are associated with a decreased number of dendritic spines. The following section summarizes a few of the main neurological disorders that have been shown to involve a marked reduction in the number of dendritic spines in different regions of the brain.

1.3.1 Parkinson's Disease

Post-mortem studies of patients with Parkinson's Disease have revealed significant loss of dendritic spine density of medium spiny neurons in the putamen and the caudate nucleus (MacNeill et al., 1988; Stephens et al., 2005; Zaja-Miltatovic et al., 2005). Dopamine fibers that degenerate primarily in Parkinson's Disease normally form synapses on the neck region of dendritic spines, while heads of dendritic spines form synapses with cerebral cortical afferent fibers. Loss of dendritic spines therefore disconnects the cerebral cortex from the basal ganglia, contributing to the motor deficits associated with Parkinson's Disease. In animal studies of Parkinson's Disease, neurodegeneration of dendritic spines is seen in otherwise healthy aged rhesus monkeys, suggesting that spine density may decrease over the lifespan (Villalba et al, 2009).

1.3.2 Alzheimer's Disease

In the early 1990s, two studies showed that Alzheimer's Disease is associated with a loss of synapses, and that this loss was directly correlated with the extent of cognitive impairment (DeKosky & Scheff, 1990; Terry et al., 1991). Moreover, these studies also showed that the loss of synapses in Alzheimer's patients was more directly correlated with cognitive impairment than the burden of ß-amyloid plaque; a neuroanatomical

feature associated with Alzheimer's Disease, which was originally thought to be the best predictor of cognitive decline (Terry et al., 1991). Later studies showed that this synaptic loss was specifically occurring in the CA1 region of the hippocampus, demonstrating the effects of synaptic loss on memory deficits (Merino-Serrais et al., 2013; Scheff et al., 2006). Dendritic spine loss in Alzheimer's patients has been shown to occur prior to the loss of neurons in these patients; findings which show the important role that dendritic spine loss plays in the early stages of this disease (Scheff et al., 2006).

1.3.3 Schizophrenia

The neuropathology of schizophrenia is incredibly complex, which is reflected in the manifestations of the disorder. It is well established that schizophrenia patients have reduced gray matter volume in multiple brains regions, such as the insula cortex (Fornito et al., 2009; Glahn et al., 2008), superior temporal gyrus (Honea et al., 2008), medial temporal lobe (Garey et al., 1998), anterior cingulate gyrus (Ellison-Wright & Bullmore, 2010; Fornito et al., 2009; Glahn et al., 2008), and the medial and inferior frontal gyri (Konopaske et al., 2014). The cause for the reduction in gray matter is not completely understood; however, post-mortem studies have shown that the reduction in gray matter in the PFC in people with schizophrenia is largely due to decreased dendritic spine density compared to healthy controls (Glantz & Lewis, 2000; Konopaske et al., 2014). The decreased density of dendritic spines in the dlPFC has been thought to underlie the cognitive deficits of schizophrenia such as executive function and working memory. Additionally, schizophrenia is associated with a decrease in dendritic spine density in the auditory cortex (Sweet et al., 2008), hippocampus (Kolomeets et al., 2005) and striatum (Roberts et al., 1996). Disruptions in connectivity in brain regions are thought to play important roles in the presentation of multiple symptoms of schizophrenia. For example, the cognitive symptoms of schizophrenia have been shown to be associated with disrupted thalamocortical projections, specifically from the medial dorsal nucleus of the thalamus to the dlPFC, which synapses on dendritic spines of pyramidal neurons (Anticevic et al., 2013; Giraldo-Chica et al., 2017).

1.3.4 Other neurological disorders

Interestingly, similar to schizophrenia, post-mortem studies on patients suffering from major depressive disorder and anxiety show a loss of dendritic spines in the dlPFC, as well as in the hippocampus (Kang et al., 2012; Soetanto et al., 2010). Additionally, post-mortem studies have shown that patients with bipolar disorder have a lower dendritic spine density in the dlPFC (Konopaske et al., 2014), once again similar to the spine pathology seen in schizophrenia. Furthermore, rodent models have shown that chronic stress causes a decrease in dendritic spine density in the mPFC (Goldwater et al., 2009; Radley et al., 2006), as well as in the anterior cingulate cortex and the hippocampus (Kassem et al., 2013). Animal models have also shown that dendritic spine density in the cerebral cortex is significantly decreased following ischemic stroke (Akulinin et al., 1997; Zhang et al., 2005).

1.4 Cognitive deficits in schizophrenia

Schizophrenia is a severe psychotic disorder consisting of positive, negative, and cognitive symptoms. Some of the positive symptoms of schizophrenia include hallucinations and delusions, whereas anhedonia and flat affect represent its negative symptoms. Numerous clinical studies have identified that the cognitive symptoms of schizophrenia include attention and memory deficits, as well as deficits in executive function. It is important to emphasize that, while patients currently have access to treatments for the positive and negative symptoms, no satisfactory treatment exists to alleviate the cognitive deficits associated with schizophrenia (Iwata et al., 2015; Kantrowitz et al., 2015; Talpos, 2017).

Overall, deficits in executive function can cause severe impairments to the quality of life of patients with schizophrenia, as well as their families. In humans, deficits in executive function can be investigated using the Wisconsin Card Sorting Task (WCST) – a behavioral paradigm which requires cognitive flexibility – in which subjects are required to match cards based on either the shape, size, number, or color of the images that appear on each card. During task performance, the subjects are not explicitly told which rule to follow to sort the cards, but by being told whether their match was correct/incorrect, they

can use these ongoing cues to eventually learn the correct sorting rule. Once they have learnt how to correctly match the card pairs (i.e., they learn the first 'set'), the rule changes and once again, they are required to follow cues in order to unlearn the previous rule and learn the new rule (Milner, 1963; Nelson, 1976). Thus, the WCST requires subjects to display cognitive flexibility in the form of their set-shifting ability. Patients with schizophrenia make more perseverative errors on this task, meaning that they have a difficult time abandoning (i.e., unlearning) the previously learned rule and adopting the new rule (Everett et al., 2001; Haut et al., 1996; Koren et al., 1998; Li, 2004).

To investigate cognitive flexibility and perseverance in rodent models, various behavioral tasks (i.e., digging; lever-pressing; swimming directions) have been designed that require the animal to display evidence of their set-shifting ability. In the lever-pressing tasks of set-shifting, instead of attempting to match cards like in the WCST, the rodents undergo appetitive conditioning to learn to press a lever associated with a given light cue by receiving a sugar pellet each time they press the correct lever. Once they have learnt this initial rule, the experimenter shifts the task requirements, and the rodent must now abandon the original rule while also learning the new rule (e.g., to only press the lever on the left or right), while ignoring the light cue (Floresco et al., 2008). Consistent with the WCST, lever-pressing tasks such as this ultimately require the rodents to show cognitive flexibility and avoid perseverating on the initial rule when it is no longer rewarded. Rodent models that seek to investigate the cognitive deficits associated with schizophrenia have been able to replicate the key findings seen in humans with schizophrenia, most notably an increased number of perseverative errors made on tasks requiring set-shifting (Broberg et al., 2008; Desai et al., 2017; Flagstad et al., 2004; Placek et al., 2013).

fMRI studies have shown that the cognitive deficits in schizophrenia patients are associated with a decreased gray matter volume in the dlPFC (Rüsch et al., 2007). Furthermore, studies of post-mortem brains have shown that this decrease in gray matter volume in schizophrenia is associated with a decreased dendritic spine density on basilar dendrites of layers 2/3 pyramidal cells in the dlPFC (Glantz & Lewis, 2000; Konopaske et al., 2014). Unfortunately, treatment efficacy of the cognitive deficits is largely affected

by the emergence of schizophrenia symptoms past the point of major cortical plasticity (Gogtay et al., 2011; Sheu et al., 2019).

In order to develop a treatment for the cognitive deficits of schizophrenia, it is crucial to choose a proper animal model that recapitulates the positive, negative, cognitive, and neuroanatomical abnormalities seen in schizophrenia. Multiple conventional models displaying schizophrenia-like symptoms are routinely used in studies of schizophrenia (e.g., PCP, amphetamine, isolation rearing, DISC1 knockout); however, none of these models represent the neurodevelopmental nature of adult-onset symptomology observed in schizophrenia, as well as a loss of spines in the mPFC and deficits in cognitive abilities associated with this brain region (reviewed in Jones et al., 2011). A neurodevelopment model showing schizophrenia-like symptoms was developed in Dr. Rajakumar's lab by causing cell death of the subplate cells, which are required for guiding proper thalamocortical projections during development. The subplate cells are lesioned by infusing nerve growth factor (NGF) into the developing PFC on postnatal day 1, which causes disrupted thalamocortical projections in these rats. As noted in previous publications from Dr. Rajakumar's lab, these subplate lesioned rats show behavioral and neuroanatomical deficits in adulthood that are consistent with schizophrenia. For example, subplate lesioned rats show impaired prepulse inhibition (Rajakumar et al., 2004), decreased social interaction (Lazar & Rajakumar, 2008), and increased perseverative errors on a set-shifting task (Desai et al, 2017). In addition to these behavioral deficits, neuroanatomical abnormalities such as ventricular enlargement, loss of neuropil in the PFC, and neuronal loss in the hippocampus have been shown in subplate lesioned rats, all of which are known to occur in the schizophrenic brain (Rajakumar & Rajakumar, 2004). Importantly for this thesis, subplate lesioned rats show decreased dendritic spine densities on layers 2/3 pyramidal cells in the prelimbic area of the mPFC; a hallmark of the neuroanatomical pathophysiology in schizophrenia patients.

1.5 Growing new dendritic spines

Since dendritic spine loss is a hallmark of many neurological disorders, growing new dendritic spines has been an important aspect of developing new treatments for these disorders. Related to this, many researchers are also working on developing new ways to

slow dendritic spine loss throughout the brain. The following section will summarize some of the main publications attempting to slow dendritic spine loss and grow new dendritic spines.

1.5.1   Antidepressants

In 2005, Hajszan and colleagues conducted a study in which they administered fluoxetine to ovariectomized female rats for both 5 days and 14 days in an attempt to increase dendritic spine density in the CA1 and CA3 regions of the hippocampus. They found that after 5 days of treatment with fluoxetine, there was a 68.8% increase in dendritic spine density in CA1 and a 19.8% increase in spine density in CA3. After 14 days of treatment, they found a 68.5% increase in spine density in CA1 and a 61.4% increase in spine density in CA3. These results suggest that the antidepressant fluoxetine may be working to increase dendritic spine density in the hippocampus of individuals with depression. Although there was a significant increase in the number of dendritic spines in these areas of the hippocampus, the overall size of the CA1 and CA3 regions did not increase, suggesting a progression of neuropil loss (Hajszan et al., 2005).

Additional studies have found that antidepressant doses of ketamine also increase dendritic spine formation in layer 5 of the PFC (Li et al., 2010). These results are promising in attempting to grow new dendritic spines in the hippocampus and the PFC; however, antidepressants (especially ketamine) can have adverse effects such as perceptual disturbances, confusion, elevations in blood pressure and dizziness (Zarate Jr et al., 2006). Thus, if the primary goal of therapy is to increase the density of dendritic spines, there may be other effective pharmacological approaches, as discussed below.

1.5.2   Rosiglitazone

Studies using the antidiabetic drug rosiglitazone were first conducted in response to findings that indicated an association between insulin resistance and Alzheimer's Disease (Craft et al., 1993; Steen et al., 2005). Rosiglitazone is a peroxisome proliferator-activated receptor-γ (PPAR-γ) agonist that acts as an insulin sensitizer as well as a mitochondrial activator. Past studies have shown that rosiglitazone was able to increase cognitive abilities in patients with mild to moderate Alzheimer's Disease (Day, 1998;

Feinstein et al., 2005; Watson et al., 2005). Furthermore, a preclinical study found that rosiglitazone reversed dendritic spine loss caused by administration of apolipoprotein E4 (a major risk factor for Alzheimer's Disease) in rat primary cortical neurons (Brodbeck et al., 2007). More specifically, they found that rosiglitazone increased dendritic spine density in these cortical neurons by 58.5%. As this positive effect was abolished when a PPAR-γ antagonist was present, these authors suggested that rosiglitazone influences dendritic spines by activating the PPAR-γ pathway (Brodbeck et al., 2007).

Interestingly, a double-blind, placebo-controlled pilot trial was conducted by Yi and colleagues in 2012 to determine the effects of rosiglitazone administration to clozapine-treated patients with schizophrenia on cognitive deficits. This pilot study tested performance on multiple behavioral tests of cognition (including the WCST) at baseline, then again after 8 weeks of treatment with either rosiglitazone or placebo. This study showed that there were no differences on performance on any of the tested cognitive tasks between the rosiglitazone-treated patients compared to placebo-treated patients, suggesting that rosiglitazone does not improve cognitive function in schizophrenia patients (Yi et al., 2012). This study provides an insightful view on the importance of the development of a novel treatment for the cognitive deficits in schizophrenia, and further demonstrates that this is an area of schizophrenia treatment that has interested other researchers.

1.5.3   Chelerythrine

Protein kinase C (PKC) signaling has been shown to cause dendritic spine collapse (Calabrese & Halpain, 2005). Due to the disrupted function of molecules associated with PKC inhibition, it is thought that excessive PKC signaling occurs during chronic stress and in people with certain mental illnesses, possibly acting as one of the contributors for the decrease in dendritic spine density, particularly in the PFC (Arnsten & Manji, 2008; Baum et al., 2008; Mirnics et al., 2001). The relationship between PKC and dendritic spine loss was directly investigated in a preclinical study conducted in 2009, in which Hains and colleagues used chelerythrine, a PKC inhibitor, to decrease dendritic spine loss in layers 2/3 pyramidal cells in the PFC during a repeated stress paradigm. In this study, rats received systemic injections of chelerythrine every day prior to undergoing a daily

stress paradigm. The results showed that chelerythrine was successful in preventing dendritic spine loss by approximately 50% (i.e., 50% of dendritic spines were protected compared to control animals) (Hains et al., 2009).

1.5.4   Glutamate modulation

The primary cause of dendritic spine loss in striatal medium spiny neurons in Parkinson's Disease is a loss of dopamine inhibitory control (through D2 receptors) over corticostriatal glutamate release (Day et al., 2006). That said, dopamine replacement therapy in patients with Parkinson's Disease, as well as animal models, does not reverse this dendritic spine loss, suggesting that simply regulating dopamine signaling through D2 receptors is not sufficient to increase dendritic spine density (Deutch et al., 2007).

A study conducted by Garcia and colleagues in 2010 aimed to directly manipulate corticostriatal glutamate release in an attempt to reverse dendritic spine loss in an animal model of Parkinson's Disease. This was accomplished by producing focal motor cortex lesions, and it was found that lesioned animals had 50% more dendritic spines in striatal medium spiny neurons compared to sham lesioned animals. Additionally, this study found that when a glutamate suppressor (mGluR2/3) agonist was used to treat cultured medium spiny neurons prior to dopamine denervation of the cultures, dendritic spines were significantly protected against spine loss. The results of this study suggest that directly suppressing corticostriatal glutamate release rather than manipulating dopamine release reverses dendritic spine loss caused by lack of dopamine inhibitory control. While these results are promising, they are limited to medium spiny neurons and Parkinson's Disease, as they are directly reversing spine loss induced by mechanisms specific to striatal medium spiny neurons.

1.5.5   PAK inhibitors

Schizophrenia is a complex neurological disorder characterized by a marked reduction in dendritic spine density in the PFC and in the auditory cortex (described above). Although there are many genetic factors involved in the loss of dendritic spines in schizophrenia, one of the most common factors is Disrupted-in-Schizophrenia-1 (DISC1), which generates pathophysiologically similar dendritic spine abnormalities to those seen in

schizophrenia when it is knocked down (Hayashi et al., 2010; Lee et al., 2011). To better understand the causal relationship between DISC1 and dendritic spine loss, Hayashi-Takagi and colleagues (2014) conducted a preclinical study using a model of DISC1 knockdown mice. In this study, a major target of Rac1 (an NMDA-type receptor that is regulated by DISC1) called p21-activated kinases (PAKs) were inhibited. Treatment with PAK inhibitors significantly increased the size of dendritic spines in the PFC of DISC1 knockdown mice and caused a trend for increasing the density of dendritic spines in this area. While these results appeared promising for reversing dendritic spine deterioration in the PFC in schizophrenia, the spine density results did not reach the level of statistical significance.

1.6   Paired Immunoglobulin-like Receptor B

Paired Immunoglobulin-like Receptor B (PirB) is a myelin-associated regulatory immune receptor. PirB is expressed in multiple neuronal types, and neuronal PirB has been shown to be involved in inhibition of dendritic spine growth. The major ligand that binds to neuronal PirB is major histocompatibility complex class 1 (MHC1), which is regulated by neuronal activity and required for normal synaptic plasticity (Huh et al., 2000). When a ligand binds PirB, its immunoreceptor tyrosine-base inhibitory motif (ITIM) becomes phosphorylated. Once this occurs, phosphatases are recruited to the ITIM of PirB, causing dephosphorylation of ERK. Decreased ERK signaling results in an overall decrease in dendritic spine density (**Fig. 4**) (Syken et al., 2006; Takai, 2005).
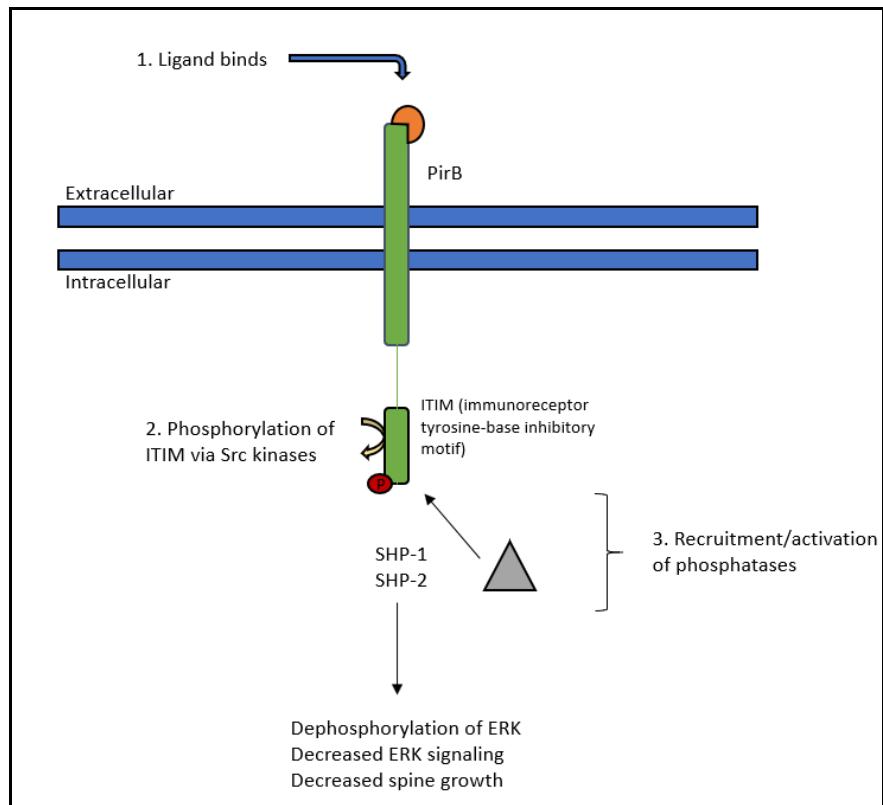
Figure 4. **Pathway by which PirB functions to inhibit dendritic spine growth.**
A ligand (e.g., NogoA, MHC-I, MAG) binds to PirB, causing phosphorylation of
the ITIM. This initiates the recruitment and activation of phosphatases SHP-1 and
SHP-2 which then dephosphorylate ERK, resulting in decreased ERK signaling
and downstream inhibition of dendritic spine growth.

Importantly, recent studies have shown that pharmacological inhibition of PirB activity
leads to dendritic spine growth in the area in which it was blocked. As described below,
these studies have also shown improvements in multiple deficits (e.g., ocular dominance
plasticity; ischemia-related memory deficits) that are associated with a loss of dendritic
spines. Overall, the final section of this chapter summarizes the current work that has
been conducted on increasing spine growth by blocking PirB activity in multiple brain
regions.

1.6.1   Blocking PirB in the visual cortex

A study conducted by Syken and colleagues in 2006 showed that PirB works to inhibit synapse growth in the visual cortex. To determine the function of neuronal PirB, a mutant mouse was generated lacking the exons responsible for encoding the transmembrane and part of the intracellular domain of PirB, making it unable to transfer signals across the plasma membrane. To test the synaptic changes associated with mice lacking functional PirB, ocular dominance (OD) plasticity was tested. The primary visual cortex primarily receives monocular inputs from the contralateral eye; however, there is a small region of binocular vision called the binocular zone (BZ) that receives inputs from both the contralateral and the ipsilateral eye. OD plasticity in the visual cortex can be assessed by examining changes in the size of the binocular zone. Syken et al., (2006) used the activity-regulated immediate-early gene Arc to determine the size of the binocular zone and found that mice lacking functional PirB had an increase in the Arc signal in layer 4 of the primary visual cortex from 22% to 54% compared to wild-type mice, indicating for the first time that PirB blocks experience-dependent synaptic plasticity beyond the critical period of plasticity.

In 2013, a study conducted by Djurisic and colleagues looked further at the inhibition of synapse formation and found that this was caused by a lack of dendritic spine growth. This study tested PirB-/- mice on a form of OD plasticity called monocular deprivation, which was previously shown to increase dendritic spine density on layer 5 pyramidal neurons of the visual cortex (Hofer et al., 2009). The PirB-/- mice had significantly more dendritic spines on layer 5 pyramidal cells compared to wild-type mice, as well as higher-frequency miniature synaptic currents, and larger long-term potentiation, all of which suggested that knocking out PirB increased the density of functional dendritic spines in the visual cortex.

Following the publication of the results by Djurisic et al. (2013), a study was conducted by Vidal and colleagues in 2016 to look more closely at the role of PirB in neurons, and the mechanisms by which it inhibits dendritic spine growth in the visual cortex. By generating mice with a conditional allele of PirB, they were able to delete PirB *in vivo* in only a subset of neurons by *in utero* electroporation of Cre recombinase. In doing so, they

found that in layers 2/3 pyramidal cells in the visual cortex, PirB has a neuron-specific and cell-autonomous effect on dendritic spine density (Vidal et al., 2016).

Finally, a recent study conducted in 2017 by Bochner and colleagues investigated the behavioral effects of blocking PirB in the visual cortex of adult mice with deprivation-induced amblyopia (i.e., impaired vision in one eye). Importantly, not only did the dendritic spine density increase in the contralateral visual field upon locally blocking PirB in the visual cortex, but this therapeutic approach resulted in the partial recovery of the impaired visual acuity associated with amblyopia. Collectively, the exciting results of this study confirm that the dendritic spines that were able to grow following the pharmacological inhibition of PirB went on to become part of functional synapses, and that these neuroanatomical changes ultimately helped to restore visual acuity in adult mice that had undergone long-term monocular deprivation.

1.6.2   Blocking PirB in the hippocampus

In 2017, Mi and colleagues conducted a study in which PirB levels were observed across different ages of mice. Their results showed that PirB expression increases in the hippocampus, cerebellum and cerebral cortex in mice as they age. Furthermore, this study showed that performance on the Morris water maze task decreased as the mice got older; findings associated with age-related impairments in spatial learning and memory. When PirB blocker was infused into the hippocampus, performance on the Morris water maze task improved compared to age-matched mice who had received a control infusion. Ultimately, these results suggest that, similar to previous studies of the visual cortex, blocking the activity of PirB in the hippocampus resulted in improved behavioral outcomes, in this case involving plasticity in the hippocampus in aged animals.

A study conducted in 2017 by Li and colleagues used a novel protein called TAT-PEP (a PirB blocker with a TAT sequence for penetration of the blood brain barrier) in the hippocampus of mice following transient global cerebral ischemia, which was done by bilateral common carotid artery occlusion (BCCAO). The results of this study showed that blocking PirB in the hippocampus following BCCAO increased performance on the Morris water maze task, step-down passive avoidance task, and the T-maze task,

compared to mice who had not received TAT-PEP. Furthermore, the authors found that following BCCAO, hippocampal cells had significantly less neurite outgrowth compared to healthy control mice. Following administration of TAT-PEP, this decrease in outgrowth was completely ablated and returned to baseline levels, suggesting that blocking PirB increased the outgrowth of neurites to normal levels in mice following cerebral ischemia.

Overall, given that blocking PirB in the hippocampus was found to significantly increase performance on tasks of both short-term and long-term memory in aged mice (Mi et al., 2017), as well as in mice who had undergone transient global cerebral ischemia (Li et al., 2017), the pharmacological blocking of PirB represents a promising therapeutic approach aimed at reversing and/or protecting against cognitive decline following aging and stroke.

1.7   Thesis Rationale, Objective and Hypothesis

As discussed above, PirB has recently been shown to play an active role in inhibiting cortical plasticity in the adult brain (Djurisic et al., 2013; Mi et al., 2017; Syken et al., 2006; Vidal et al., 2016). In addition, studies have shown that blocking PirB in adult rodents can enhance spine growth in the visual cortex, resulting in functional recovery of amblyopia (Bochner et al., 2017; Djurisic et al., 2013). Given that leading explanations for the basis of altered cognition in schizophrenia focus on a decrease in glutamatergic transmission in the PFC, and in turn a reduction in the number of dendritic spines, blocking PirB holds great promise for both initiating cortical plasticity in adulthood and increasing cognitive function.

Evidence described above indicates that blocking PirB function facilitates growth of dendritic spines in primary sensory areas. However, it is not known whether a similar effect would occur in association cortices, especially in multimodal association cortex such as the PFC. In the present thesis, it was **hypothesized** that PirB inhibits dendritic spine growth in the rodent mPFC in adulthood such that blocking its activity will increase dendritic spine density in the mPFC. The **objective** of this thesis was to molecularly assess the ability of PirB blocker to enhance dendritic spine density in the prelimbic area

of the mPFC of an established animal model that recapitulates several neuroanatomical changes and behavioral deficits associated with schizophrenia.

1.8 Experimental Series

In order to test our hypothesis, we used subplate lesioned rats, which are a neurodevelopmental model that show schizophrenia-like symptoms (including spine loss on basilar dendrites of layers 2/3 pyramidal cells in the prelimbic area) in adulthood (described in section 1.4). In order to increase the loss of dendritic spines in the PFC, the neonatally lesioned rats were subjected to repeated unpredictable and mild stressors during their adolescent period. This two-hit model showed a robust reduction in dendritic spine density throughout the layers of the PFC and therefore provided a suitable animal model to test our hypothesis that blocking PirB will facilitate dendritic spine growth in the PFC in adult animals. We employed a within subject design as each animal received PirB blocker into one side of the PFC, while the contralateral PFC was infused with the vehicle, and both sides were processed and analyzed simultaneously and identically.

As noted above, the objective of this thesis was to examine the effects of blocking PirB in the prelimbic area of subplate lesioned and adolescent stressed rats. To that end, a series of experiments were conducted in which bilateral cannulae were chronically-implanted into the prelimbic area of the mPFC of these rats, so that the PirB blocker could be repeatedly micro-infused into the left hemisphere and sterile phosphate buffered saline (PBS) into the right hemisphere; an experimental approach that allowed each rat to serve as its own control. Upon completion of the infusion protocols, rats were transcardially perfused, and the brains were harvested, and ultimately stained for histological analysis in accordance with the specific aim of the experimental series (outlined below).

The Experimental Series addressed three specific aims:

1) **Confirm the location of the cannula implantation using rhodamine and NeuroTrace (a fluorescent Nissl stain) counterstaining.** This was achieved by infusing the red fluorescent dye rhodamine into the prelimbic area of a subset of rats that had received bilateral cannulae implantations. Once these rats were

perfused and brains were sliced, they were counterstained with the green fluorescent Nissl stain, NeuroTrace. The slices were then imaged using fluorescent microscopy and compared to a rat brain atlas to confirm that the rhodamine was present in the prelimbic area only.

2) **Quantify dendritic spine densities on layers 2/3 pyramidal cells along individual dendrites in the prelimbic area following PirB blocker infusions using the Golgi-Cox method.** The second objective of this thesis was conducted by Golgi-Cox impregnation of the brain slices that had undergone infusions of both PirB blocker and PBS. As Golgi-Cox impregnation only labels less than 10% of whole neurons, this improves the quantification of dendritic spine density (Zaqout & Kaindl, 2016). Ultimately, this technique allowed us to quantify the number of dendritic spines in each of the two hemispheres, and to perform statistical analyses to compare them to each other.

3) **Examine the overall differences between the PirB-infused hemisphere and the PBS-infused hemisphere on a global scale using immunohistochemistry labelling of Neurabin-2.** The final objective in this thesis was to gain a global understanding of the effects of blocking PirB in the prelimbic area. As previously discussed, Golgi-Cox impregnation randomly labels less than 10% of neurons. For this reason, we wanted to ensure that any effects shown in the previous objective were not simply occurring in the random sample of labelled neurons, but rather were occurring at a global level. In order to test this objective, immunohistochemistry was conducted to label Neurabin-2, a scaffolding protein that is concentrated in dendritic spines (Satoh et al., 1998). This objective, combined with the previously described objective, allowed us to examine how blocking PirB function affects spine density at individual neurons, as well as on the larger population of layers 2/3 pyramidal neurons in the prelimbic area.

Chapter 2

2   Materials and Methods

2.1   Animals

The experiments in this thesis were conducted to assess the effects of blocking PirB in the prelimbic area of the mPFC in our two-hit rat model that shows positive, negative and cognitive symptoms consistent with schizophrenia. All experiments employed neonatally subplate lesioned (first hit) rats that were then subjected to chronic mild psychological stressor during adolescence (second hit). Adult animals underwent stereotaxic bilateral cannulae implantation surgery. Ten animals (8 females; 2 males) underwent subplate lesioning and stress exposure, and another three animals (females) were sham lesioned and not stressed. All 13 animals underwent surgery for bilateral cannulae implantation. All experiments used Sprague-Dawley rats (Charles River Laboratories, Inc., Wilmington, MA, USA) that were housed in a temperature-controlled room with a 12 h light–dark cycle. The day of birth was considered postnatal day 0, and all rats were given food and water *ad libitum* throughout all experiments. All experimental procedures were approved by the University of Western Ontario Animal Use Subcommittee and were in accordance with the guidelines established by the Canadian Council on Animal Care. All efforts were made to reduce the number of animals used and to minimize pain felt by the animals.

2.2   Nerve Growth Factor Infusions

Infusions of nerve growth factor (NGF) were administered on postnatal day 1 following protocols by Rajakumar et al. (2004). Half of the pups in each litter were randomly selected and separated from their mother for up to 10 minutes, while the other half remained with the mother. One by one, pups were placed under a heat lamp, and bregma was visualized through the scalp. Bilateral stereotaxic injections of 0.5 µL NGF (human recombinant NGF; 125 ng/µL in sterile saline) were administered into the developing frontal cortex at +1.0 mm rostrocaudal, -1.5 mm dorsoventral, and both + 0.5 and - 0.5 mediolateral from bregma. Injections were done using a 30 G needle (custom made to

penetrate the skin by 1.5 mm) connected to a 10 µL Hamilton syringe by Teflon tubing. Pups received a cut to their left ear following NGF injections for identification. Once the final injection was complete, the pups were returned to the mother. During the injection procedure, pups were never separated from their mother for more than 10 minutes. The second half of the litter underwent the same general procedures; however, instead of NGF infusions, they received infusions of physiological saline, and they received a cut to their right ear for identification. For each pup, the infusion procedure was repeated on postnatal day 2. For the experiments discussed in the current thesis, only three saline-infused (i.e., sham-lesioned) rats were used, while the remainder of these rats were used for other experiments in the lab. Animals used in the current study were from 3 different litters and were randomly selected, while the remaining animals were employed in parallel studies in the laboratory.

2.3 Stress exposure during adolescence

On postnatal day 32, ten rats in the NGF-infusion group experienced their 'second hit' which included exposure to non-traumatic, mild psychological stressors twice per day for 14 consecutive days. This stress model was chosen because it is known to cause significant loss of dendritic spine densities throughout the cerebral cortex. During the 14 consecutive days, the rats were exposed to different types of stressors in a random order; an approach that made the stressors unpredictable to the rats. The types of stressors used were as follows: wet cage, forced swimming, overnight light exposure, and overnight social isolation. The wet cage stressor involved subjecting rats to 1.5 L of water in a 45º tilted cage for 20 minutes. The forced swimming stressor involved placing a rat for 15 minutes in a tall tub that was filled with water (15ºC), which required them to swim for the duration as they could not touch the floor or reach the brim of the tub. The overnight light exposure stressor involved maintaining a well-lit environment overnight, as well as removing any objects in the cage that rats could use to hide from the light. The social isolation stressor involved separating rats from their cage mates, and housing them individually overnight. Following the 14-day stress period (from postnatal day 32 - 46), the adolescent rats were left undisturbed in their home cages until postnatal day 63, which is considered adulthood in rats.

2.4   Bilateral cannulae implantation

On postnatal day 70 - 80, rats underwent stereotaxic surgery for bilateral cannulae implantation. Prior to the surgery, rats were deeply anesthetized using isoflurane (4% for induction, 2% for maintenance; Baxter Corporation, Mississauga, ON), and throughout the procedure, their body temperature was monitored and maintained at ~37ºC using a homeothermic heating pad. Once anesthetized, rats were placed in a stereotaxic frame and received Metacam (1mg/kg, subcutaneously) and Baytril (10mg/kg, subcutaneously). Next, a central incision (2.5 cm) was made in the scalp, and the underlying fascia was removed to expose the skull. Two small holes for the cannulae were drilled into the skull at -3.2 mm rostrocaudal to Bregma and either +0.8 mm or -0.8 mm mediolateral to Bregma (Paxinos & Watson, 2006). Two slightly larger holes were then drilled caudal to Bregma on either side of the central line and bone screws were gently screwed into the skull to ultimately serve as anchors for the cannulae implantation. Next, using a stereotaxic arm, 27G guide cannulae (RWD Life Sciences Inc., San Diego, CA) were carefully inserted through the drill holes until the tips were located slightly dorsal to the prelimbic area of the mPFC (-1.5 mm dorsoventral to Bregma; Paxinos & Watson, 2006). Internal stylets were placed inside the guide cannulae to prevent fluid from blocking the cannulae. Dental cement was then applied onto the skull, covering the bone screws and the base of the cannulae. Once the dental cement had hardened, the excess skin around the incision was trimmed, and the wound was closed following standard suturing procedures. Finally, animals received a 4 mL bolus of saline to rehydrate, and the isoflurane was turned off. Animals received Metacam (1mg/kg, subcutaneously) and Baytril (10mg/kg, subcutaneously) for three days following surgery. During this time, the rat's body mass, behavior and overall appearance were monitored closely to ensure its health and welfare. For the week following the surgery, each rat was allowed to recover in a separate cage, so as to avoid damage to its chronic implant via a cage mate.

2.5   Confirmation of stereotaxic location of the infusion site

The first objective was to confirm the location of the cannulae following the implantation surgery. Overall, this was achieved by infusing the red fluorescent dye rhodamine into the prelimbic area, then counterstaining the brain with the green fluorescent Nissl stain

NeuroTrace. Ultimately, the fluorescent images were then compared to a rat brain atlas in order to confirm that the stereotaxic location of the cannulae resulted in an infusion into the prelimbic region of the mPFC. This procedure was repeated on three rats (n = 3).

2.5.1   Rhodamine infusions

One week after the last cannulae implantation surgery, animals received intra-cerebral infusions of the red fluorescent dye rhodamine. In order to avoid stressing or harming the rats during infusions, each rat was lightly anesthetized using 4% isoflurane (Baxter Corporation, Mississauga, ON) for two minutes prior to removing the internal stylet. Once anesthetized, the stylet was carefully removed and the 33G, 2.0 mm long injector cannula (RWD Life Sciences Inc., San Diego, CA) attached by Teflon tubing was inserted into the prelimbic area. The infusion cannulae extended 0.5 mm beyond the tips of the guide cannulae to effectively target the prelimbic area. Rhodamine was infused into both the left and right hemispheres at a rate of 0.05 µl per minute for one minute, for a total of 0.05 µL per hemisphere.

2.5.2   Histology: Rhodamine infusions

Twenty-four hours following their rhodamine infusion, animals were deeply anesthetized with ketamine-xylazine (80 mg/kg ketamine, 5 mg/kg xylazine, intraperitoneal) until the point in which there was an absence of a pedal withdrawal reflex. At this time, the rats underwent a transcardial perfusion of 300 mL 0.9% saline followed by 400 mL 4% paraformaldehyde (Sigma-Aldrich) in phosphate buffer (pH = 7.2) at a rate of 65 mL/minute. Brains were extracted and kept in a 30% sucrose solution for 48 hours, then transferred to a 15% sucrose solution for long-term storage in 4ºC.

For tissue processing, the brains were blocked, and the frontal cortex was quickly frozen by covering in powdered dry ice for ~2 minutes. The frozen brain block was then transferred to a microtome stage (Thermo Scientific) using OCT and sliced into 40 µm thick sections. These coronal sections were mounted onto frosted slides and left to dry upright for at least 24 hours.

Once dry, slices were flooded with 100 µL of the green fluorescent Nissl stain NeuroTrace (4 µg/mL) and left for 20 minutes. The slides were then washed twice in phosphate buffer (PB, pH = 7.2) for 4 minutes, and again left to dry upright in the dark for 24 hours at room temperature. As the final step, coverslip glass was applied using Vectashield Antifade mounting medium (BioLynx Inc.), and these covered slides were allowed to dry for 10 minutes.

2.5.3 Imaging: Rhodamine infusions

Fluorescent microscopy was conducted using a Nikon Eclipse microscope, and images were captured using NIS-Elements software. Rhodamine dye was imaged using a maximum excitation wavelength of 553 nm, whereas NeuroTrace dye was imaged using a maximum excitation wavelength of 500 nm. Images were first taken of the NeuroTrace dye in order to confirm the location at 2x objective. Next, the rhodamine images were taken at 2x objective. All images were then compared to a rat brain atlas in order to confirm that the infusion targeted the prelimbic region of the mPFC (Paxinos & Watson, 2006). The confirmation of location was done on three animals (n = 3).

2.6 Quantitative assessment of dendritic spine densities along individual dendrites in layers 2/3 using the Golgi-Cox method

The second objective was to quantify dendritic spine densities in both hemispheres; one that had received infusions of the PirB blocker, and the other PBS. This was achieved by Golgi-Cox impregnation of the infused brains, allowing for imaging of whole neurons. Golgi-Cox impregnation only stains less than 10% of neurons, allowing for accurate quantification of dendritic spine densities (Zaqout & Kaindl, 2016). Spine densities on layers 2/3 pyramidal cells were counted in both hemispheres, and results statistically compared to each other in order to determine whether blocking PirB in the prelimbic area increases dendritic spine density. Golgi-Cox impregnation and analysis were conducted on 8 rats; however, staining was unsuccessful on one rat. Thus, the results of the Golgi-Cox method were analyzed for 7 rats (n = 7). For three of these 7 rats, dendrites outside of the prelimbic area were also analyzed. This was done in order to ensure that any

differences seen in the prelimbic area of the mPFC were not caused by spontaneous recovery of dendritic spines, but rather by blocking PirB activity in that area specifically.

2.6.1   PirB Blocker & PBS Infusions

One week after the cannulae implantation surgery, animals received infusions of a PirB ectodomain (PE), which acts as a decoy for competing ligands for PirB (Bochner et al., 2017). The PirB blocker (PE) and PBS were infused to the left and right hemispheres, respectively. In order to avoid stressing or harming the rats during infusions, each rat was lightly anesthetized using 4% isoflurane (Baxter Corporation, Mississauga, ON) for two minutes prior to removing the internal stylet. Once anesthetized, the stylet was carefully removed and the 33G, 2.0 mm long injector cannula (RWD Life Sciences Inc., San Diego, CA) attached by Teflon tubing 4was inserted into the prelimbic area. Again, the infusion cannulae extended 0.5 mm beyond the tips of the guide cannulae in order to effectively target the prelimbic area of the mPFC. PirB blocker (PE; 50 µg/100 µL sterile PBS) was infused into the left hemisphere while PBS alone was infused into the right hemisphere at a rate of 0.05 µL per minute for one minute, for a total of 0.05 µL per hemisphere. Infusions were done twice per day, 10 hours apart, for 5 days in order to preserve the integrity and positioning of the cannulae (Bochner et al., 2017).

Twenty-four hours following the last drug infusion, animals were deeply anesthetized with ketamine-xylazine (80 mg/kg ketamine, 5 mg/kg xylazine, i.p) until the point in which there was an absence of a pedal withdrawal reflex. A transcardial perfusion was then performed using 400 mL 0.9% saline at a rate of 65 mL/minute. No fixative was used in this step because in order for the Golgi-Cox solution (described in the next section) to properly impregnate the tissue, it must be unfixed. Brains were extracted and kept in a 30% sucrose solution for 48 hours, then transferred to a 15% sucrose solution for long-term storage in 4ºC.

2.6.2   Golgi-Cox method

Golgi-Cox impregnation was mainly conducted following the protocol by Zaqout & Kaindl, 2016; however, a few minor changes were made because the original protocol was designed for processing mouse, not rat, brain. As the first step, Golgi-Cox

impregnation solution was prepared by mixing 50 mL mercuric chloride ($HgCl_2$, 5 g/mL, Thermo Fisher Scientific) with 50 mL potassium dichromate ($K_2Cr_2O_7$, 5 g/mL, Thermo Fisher Scientific). Next, 40 mL potassium chromate (K_2CrO_4; 5 g/mL, Thermo Fisher Scientific) was added. Finally, 100 mL ddH_2O was added to the solution. The impregnation solution was left to sit in the dark at room temperature for 48 hours with no disruptions to the container to ensure that the precipitate formed on the bottom of the container was not mixed into the solution. Unfixed brains were blocked, and the frontal cortex was placed in a small tube containing ~10 mL of the Golgi-Cox impregnation solution and left at room temperature in the dark. After 24 hours, the block was removed from the tube and transferred to a new tube containing fresh Golgi-Cox impregnation solution to sit at room temperature in the dark for 10-14 days. Importantly, the impregnation solution was taken from the middle of the container to avoid taking any of the precipitate that had formed on the bottom of the container. We found that taking from the middle rather than the top of the solution provided a clearer image with less background staining of myelin.

The next step was a tissue protection step, for which a solution was prepared by dissolving 300 g sucrose ($C_{12}H_{22}O_{11}$; Thermo Fisher Scientific), 10 mL glycerol ($C_3H_8O_3$; Thermo Fisher Scientific) and 300 mL ethylene glycol ($C_2H_6O_2$; Thermo Fisher Scientific) in 500 mL phosphate buffer. The brain blocks were removed from the impregnation solution and placed in new tubes containing ~10 mL of this tissue protection solution, which were kept at 4ºC in the dark. After 24 hours, the blocks were removed from the tubes, placed in new tubes containing ~10 mL tissue protection solution, and kept at 4ºC in the dark for 10 days.

Next, the brains were sliced using an Oxford Vibratome Sectioning System. For this step, the brains were removed from the tissue protection solution and attached to a small block using cyanoacrylate adhesive (Krazy Glue). The block with the attached brain was placed inside the vibratome chamber, which was filled with remaining tissue protection solution. Slices were cut into 200 µm thick slices at a frequency of 60 Hz. The speed setting was set to 6 and the amplitude setting was set to 5; settings based on multiple attempts to slice the sections. Slices were then carefully picked up by a thin paint brush, immediately

placed on frosted slides and pressed down with a fully soaked Kim Wipe. The slides were left to dry upright for 48 hours in the dark at room temperature. The same process for sectioning was used to look at dendrites outside of the prelimbic area; however, slices were cut caudal to the injection site.

The next step was developing the Golgi-Cox impregnated slices in order to activate the reaction and make it possible to image the neurons. This was achieved by first washing the slides in distilled water twice for 5 minutes each, then dehydrating the slides in 50% ethanol for 5 minutes. The slides were then placed in a 3:1 ammonia solution (Caledon Laboratory Chemicals) for 8 minutes and washed again in distilled water twice for 5 minutes each. Once washed, the slides sat in a 5% thiosulfate solution (Sigma Aldrich) in the dark for 10 minutes, then were washed in distilled water twice for 1 minute each. Once the slides were fully developed, they underwent a series of steps in order to fully dehydrate and rehydrate prior to mounting the cover glass. They first went through an ethanol series (70%, 95%, 100% ethanol for 6 minutes each), then they were immersed in xylene for at least 6 minutes. Finally, slides were mounted using a xylene based mounting medium (Entellan; EM Science) and left to dry upright in the dark for 48 hours at room temperature.

2.6.3   Imaging: Dendritic spines

Brightfield microscopy was conducted using a Nikon Eclipse microscope, and images were captured using NIS-Elements software. Choosing dendrites for analysis was done by first finding and focusing on a cell body in the prelimbic area, then adjusting the focus on the basal dendrites. If the neuron had tertiary branching of the basal dendrites, it was used for analysis. This was done in order to ensure there was no bias in choosing dendrites for analysis. Once the dendrite was chosen, multiple images were taken at 40x objective in order to ensure that all spines along the dendrite were imaged. An image was also taken on either end of the z plane in which the dendrite was found in order to ensure that anything that was not actually a dendritic spine showed up in an image and could be excluded from the analysis. Dendritic spine length (µm) was measured using the NIS-Elements software.

Four tertiary dendrites were used from different neurons for each slice, and two slices were used for each hemisphere (i.e., 8 dendrites were analyzed for each hemisphere, for each animal). This was true for all animals except one, who had only 7 dendrites analyzed from the left hemisphere because the way in which the brain was sliced meant that only 7 dendrites with tertiary branching on the basal dendrites of layers 2/3 pyramidal cells in the prelimbic area were present. In total, 56 dendrites were analyzed in the right hemisphere (PBS infused) and 55 dendrites were analyzed in the left hemisphere (PirB blocker infused).

For dendrites outside of the prelimbic area, slices were taken from just rostral to the injection site. Dendrites were once again chosen by first focusing on a cell body in layer 2/3, then adjusting the focus until the basal dendrites became clear. Only tertiary branches of the basal dendrites were used, and dendrites were all lateral to the prelimbic area, in the primary motor cortex (M1). This analysis was conducted using 3 of the 7 animals (n = 3) and again, 4 tertiary dendrites were used from different neurons for each slice, and two slices were used for each hemisphere (i.e., 8 dendrites were analyzed for each hemisphere, for each animal). For one of the animals, only 5 tertiary dendrites were stained on layers 2/3 pyramidal cells in the prelimbic area of the left hemisphere due to how the brain was sliced, therefore a total of 24 dendrites were analyzed in the right hemisphere (PBS infused) and 21 dendrites were analyzed in the left hemisphere (PirB blocker infused).

2.6.4   Analysis: Dendritic spines

Dendritic spine densities were analyzed using ImageJ. The contrast of the images was enhanced in order to better visualize the dendritic spines, and spines were counted using the multipoint tool. Spine densities were calculated as the number of spines along a dendrite divided by the length of the dendrite.

All statistical analyses were conducted using GraphPad. A paired t-test was conducted to compare the overall average dendritic spine density in the left hemisphere to the dendritic spine density in the right hemisphere within the prelimbic area using individual spine density averages for each of the 7 animals. Paired t-tests were similarly conducted to

compare spine densities in both hemispheres outside of the prelimbic area (M1) for the overall average using individual average spine densities for each of the 3 animals. All graphs were also made using GraphPad.

2.7 Assessment of the global effect of blocking PirB in the mPFC using immunohistochemistry

The final objective was to gain an understanding of the overall effect of blocking PirB in the prelimbic area on a global level, as well as to provide confirmation that the quantitative results were consistent with results obtained by immunohistochemistry. This was achieved by immunohistochemical labelling of Neurabin-2, a protein found in dendritic spines, to view the global effects of blocking PirB in the areas in which the infusions spread. This procedure was conducted on two rats (n = 2).

2.7.1 PirB Blocker & PBS Infusions

Infusions of PirB blocker and PBS were conducted one week following the final cannulae implantation surgery, as described in the second objective (2.6.1). Twenty-four hours following their final infusion, animals were perfused, and brains were harvested and sectioned for immunohistochemistry following the methods described in the first objective (2.5.2).

2.7.2 Neurabin-2 immunohistochemistry

Once slices were dry, immunohistochemistry was conducted to stain for the synaptic scaffolding protein Neurabin-2. This was done by first applying the primary antibody. Slides were washed 4 times in phosphate buffer (PB) for 5 minutes each then placed in small tubes containing 1 mL blocking solution (100 µL/mL BSA and 100 µL/mL non-immune goat serum in PB) in order to prevent any non-specific binding. Slices were left to rotate in the blocking solution for one hour, then were washed again 4 times in PB for 5 minutes each. Next, slices were placed in a small tube containing 1 mL primary antibody (Sigma Aldrich) solution (10 µL/mL BSA, 1 µL/mL non-immune goat serum and 0.25 µL/mL rabbit antibody for Neurabin-2 in PB) to rotate overnight.

The following morning, slices were removed from the primary antibody solution and washed in PB 4 times for 5 minutes each. They were then placed in a small tube containing 1 mL of the secondary antibody (Sigma Aldrich) solution (2 µL/mL biotinylated goat anti-rabbit, 10 µL/mL BSA and 10 µL/mL non-immune goat serum in PB) to rotate for one hour. The slices were then washed again in PB 4 times for 5 minutes each then placed in a new tube containing 1 mL avidin biotin complex that had sat to combine for at least 10 minutes (2 µL/mL avidin mixed with PB, then added 2 µL/mL biotin) for signal amplification. The slices rotated in the avidin biotin complex for one hour, then were washed again in PB 4 times for 5 minutes each. Next, 1 mL of a biotinylated tyrosine solution (4 µL/mL biotinylated tyrosine in PB) was pipetted into wells in a 12-well plate. The slices were transferred to these wells and 1 µL 3% hydrogen peroxide (H_2O_2) was pipetted into each well in 30 second increments, lightly shaken, and left to sit for 10 minutes. This step was done to further amplify the signal. After 10 minutes, the slices were removed and washed with PB 4 times for 5 minutes each. Finally, the slices were placed in a new small tube containing 1 mL avidin conjugated green fluorochrome (4 µL/mL fluorescein avidin and PB) and left to rotate for one hour. The slices then went through a final series of 4 PB washes for 5 minutes each, then were mounted on frosted slides and left to dry upright in the dark at room temperature for at least 24 hours. Once the slides were dry, coverglass was applied using Vectashield Antifade mounting medium (BioLynx Inc.) and the covered slides were left to dry for 10 minutes before imaging.

2.7.3   Imaging: Neurabin-2

Fluorescent microscopy was conducted using a Nikon Eclipse microscope, and images were captured using NIS-Elements software. The fluorescein was imaged using a maximum excitation wavelength of 494 nm. Images were taken of the prelimbic area of both hemispheres at 2x objective. The two hemispheres were qualitatively compared to each other. Two animals were used for Neurabin-2 staining (n = 2).

2.7.4   Analysis: Neurabin-2

Pixel intensities were analyzed using ImageJ. For each hemisphere, a 5x5 grid of 2500 pixels (100 pixels for each individual square within the grid) was made within the

prelimbic area, as well as in the motor cortex for comparison. Average pixel intensities were calculated for each individual grid square and a ratio of pixel intensity was calculated by dividing the average pixel intensity for each individual square in the prelimbic area by its matching grid square in the motor cortex. Graphs were made using GraphPad.

Chapter 3

3 Results

3.1 Confirmation of stereotaxic location of the infusion site

The first objective was to confirm the location of the cannulae implantation. This was done by infusing the red fluorescent dye rhodamine (**Fig. 5C**) into the prelimbic area via the implanted cannula and counterstaining the brain with green fluorescent Nissl stain, NeuroTrace (**Fig. 5B**). The stained brains were then compared to a rat brain atlas to confirm the location of cannulae implantation (Paxinos & Watson, 2006) (**Fig. 5A**). **Figure 5** shows that the cannula was indeed correctly implanted in the target location (i.e., prelimbic area).
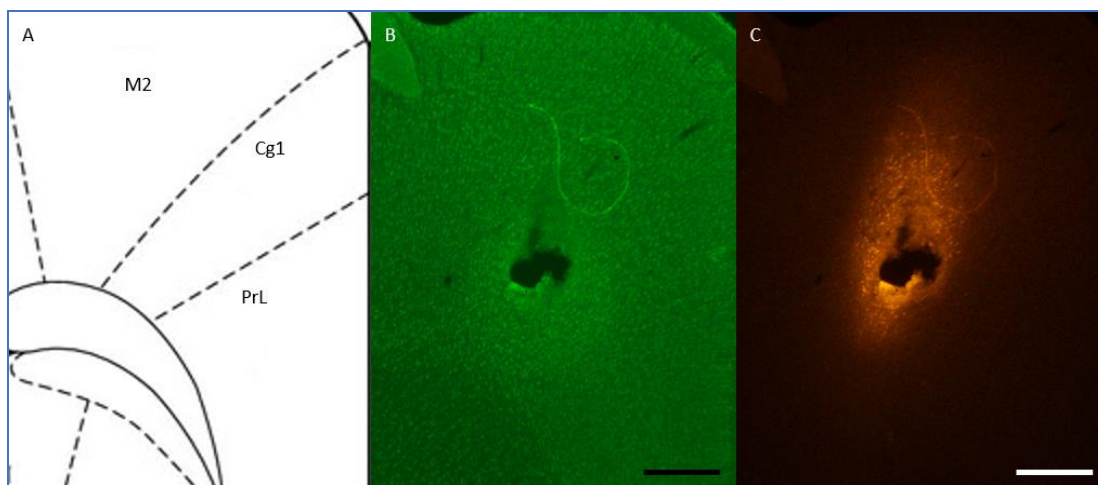
Figure 5. Confirmation of stereotaxic location of the cannula implantation and infusion site. (A) Compared to the supplementary motor cortex (M2) and the cingulate cortex (Cg1), the prelimbic area (PrL) is located more dorsal within the rat medial prefrontal cortex, as shown on a schematic of the rat brain atlas (Adapted from Paxinos & Watson, 2006). **(B)** Scaled to the same size as the atlas schematic, the representative image, which is stained for NeuroTrace, shows the location of the distal tip of the cannula in the prelimbic cortex. Note the micro-damage (tissue void)

caused by the cannula; an expected outcome with any chronic implantation. **(C)** Examining the tissue section using a different filter setting on the microscope revealed the site of rhodamine infusion in the prelimbic area of the medial prefrontal cortex; the intended target for the subsequent experimental treatments. Scale bars represent 1 mm.

3.2 Quantitative assessment of dendritic spine densities along individual dendrites in layers 2/3 using the Golgi-Cox method

The second objective of this thesis was to quantify dendritic spine densities in the prelimbic area of individual neurons. This was achieved by labelling cortical neurons in the mPFC using the Golgi-Cox method. Prior to investigating the infusion effects in the prelimbic area, neurons in M1, just rostral to the injection site, were first analyzed to ensure that changes observed were not caused by spontaneous recovery of dendritic spines, and that there were no underlying differences between the hemispheres prior to infusing the PirB blocker (PE). Next, spine densities in the prelimbic area were analyzed and compared between hemispheres to determine the effect of blocking PirB function in the prelimbic area. This was done by looking at individual spine densities for each animal across all conditions. Overall, the results of this experiment show that dendritic spine densities in M1 were the same between hemispheres regardless of the treatments to the prelimbic area, whereas spine densities in the prelimbic area were increased in the PirB blocker-infused hemisphere compared to the PBS-infused hemisphere (**Fig. 6**). Data points for each of the four conditions (right, outside prelimbic; right, inside prelimbic; left, outside prelimbic; left, inside prelimbic) are shown (outside of the prelimbic area: n = 8 for animals 1 and 3; n = 5 for animal 2; inside the prelimbic area: n = 8 for animals 1, 2, 4, 5, 6,7; n = 7 for animal 3) (**Fig. 6**).
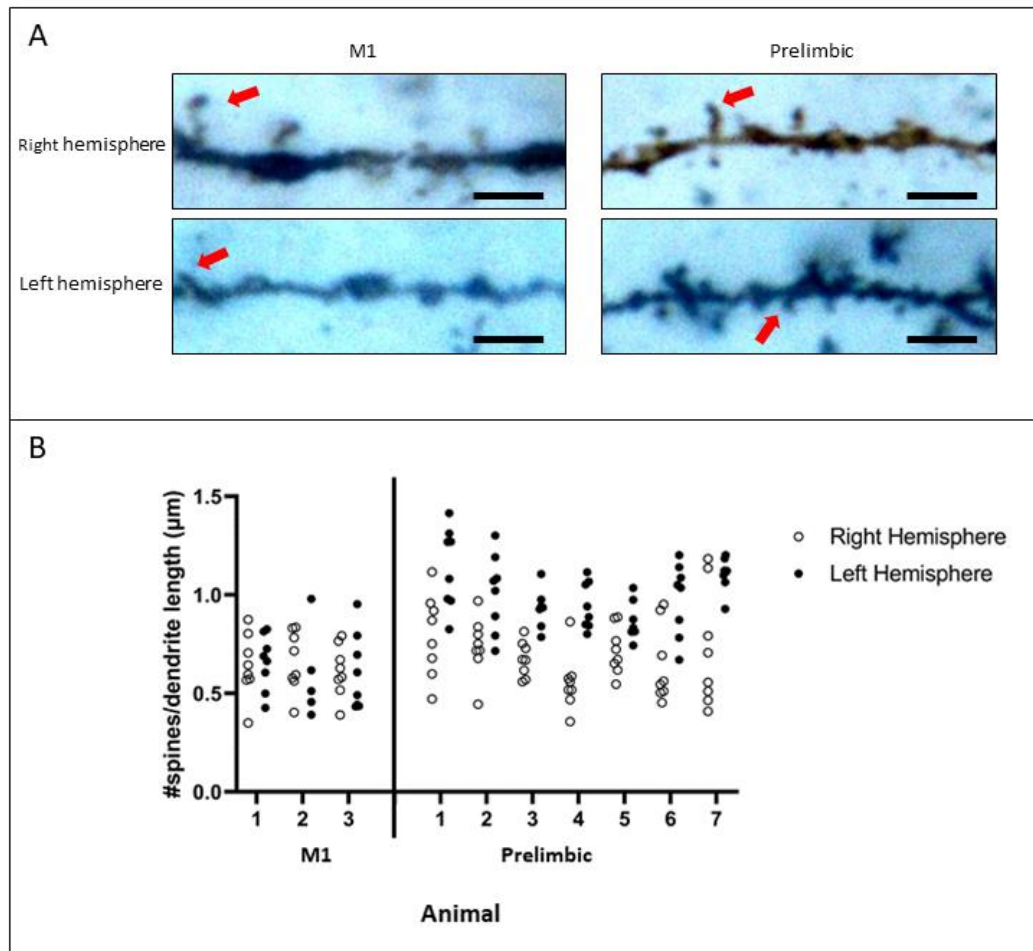
Figure 6. Raw Golgi-Cox impregnation data to assess dendritic spine densities inside and outside of the cortical area targeted by the intracerebral infusions. (A) Representative dendrites from both the right and left hemispheres, in the prelimbic area and in the primary motor cortex (M1). Red arrows are pointing to dendritic spines. Scale bars represent 10 µm. **(B)** Individual spine densities across all conditions for each animal. White circles represent individual spine densities from the right hemisphere (PBS infused), whereas black circles represent individual spine densities from the left hemisphere (PirB blocker infused). Spine densities were calculated as the number of dendritic spines along a dendrite divided by the length of the dendrite (µm). All datum points to the left of the vertical line represent spine densities from outside of the prelimbic area (i.e., M1) whereas datum points to the right of the vertical line represent spine densities inside the prelimbic area.

The average spine densities for both hemispheres of each of the three animals that had spines analyzed outside of the prelimbic area (in M1) were compared. For this experiment, each animal had 8 dendrites analyzed per hemisphere, apart from one animal that had only 5 dendrites analyzed in the left hemisphere (described above). As animal 2 only had 5 dendrites analyzed on the left side, only 5 pairs were analyzed for this section. Overall, outside of the prelimbic area, 24 dendrites were analyzed from the right hemisphere and 21 dendrites were analyzed from the left hemisphere. The overall mean dendritic spine densities for each hemisphere were compared using a paired t-test and no significant difference was found ($p = 0.5146$, $t = 0.7852$, $df = 2$) (**Fig. 7**).
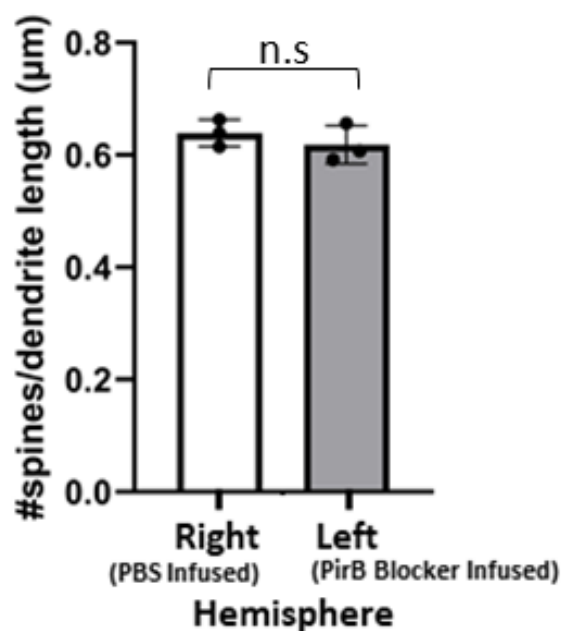
Figure 7. Average spine densities in M1, a cortical area outside of the target region of the intracerebral infusions. Spine densities were calculated as the number of spines along a dendrite divided by the length of the dendrite (μm). White bars represent mean spine density of the right hemisphere, and gray bars represent mean spine density of the left hemisphere. Error bars represent SEM. A paired t-test revealed no significant difference between the right and left hemispheres in M1 ($p = 0.5146$, $t = 0.7852$, $df = 2$). ($n = 3$ in both hemispheres).

To determine the efficacy of the PirB blocker at increasing spine density, the average spine densities for both hemispheres of each of the 7 animals that had spines analyzed within the prelimbic area were compared. For this experiment, each animal had 8 dendrites analyzed per hemisphere, apart from one animal that had only 7 dendrites analyzed in the left hemisphere (described above). Animal 3 only had 7 dendrites analyzed on the left side, therefore only 7 pairs were analyzed for this section. Overall, inside the prelimbic area 56 dendrites were analyzed from the right hemisphere, and 55 dendrites were analyzed from the left hemisphere. Ultimately, for each of the 7 rats, their mean dendritic spine densities for each hemisphere was calculated, thereby providing one value per hemisphere for each rat. These overall mean dendritic spine densities were then compared across the hemispheres using a paired t-test, and a significant difference was found ($p < 0.0001$, $t = 9.248$, $df = 6$); findings which confirmed that the PirB blocker (PE) significantly increased spine densities in the rats that underwent a neonatal subplate lesion (first hit) followed by adolescent stress (second hit) (**Fig. 8**).
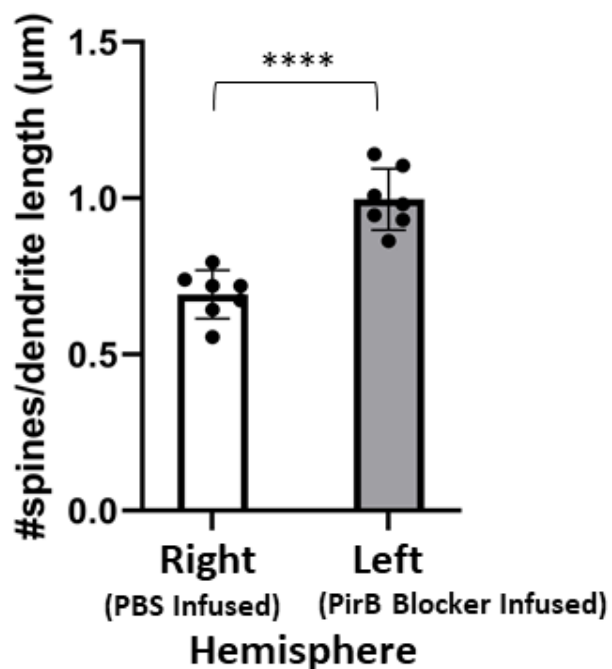
Figure 8. Average spine densities inside the prelimbic area of the medial prefrontal cortex, the region targeted by the intracerebral infusion of the PirB blocker as well as PBS. Spine densities were calculated as the number of spines along a dendrite divided by the length of the dendrite (μm). White bars represent mean spine density of the right hemisphere (PBS infused) and gray bars represent mean spine density of the left hemisphere (PirB blocker infused). n = 7 in both hemispheres; Error bars represent SEM. Compared to the PBS infusion (right hemisphere), the PirB blocker (left hemisphere) significantly increased the overall mean dendritic spine density in the prelimbic area of the medial prefrontal cortex (paired t-test: $p < 0.0001$).

3.3 Assessment of the global effect of blocking PirB in the mPFC using immunohistochemistry

The final objective of this thesis was to gain a qualitative understanding of how global dendritic spine densities change in response to blocking PirB activity in the prelimbic area. This was achieved by immunohistochemical labelling of the synaptic scaffolding protein Neurabin-2, which is concentrated in dendritic spines. The pixel intensity within the prelimbic area and outside of the prelimbic area were compared, such that the ratio for both the left and right hemispheres was determined. As a complementary approach to the Golgi-Cox quantification analysis described above, this method of analysis using the Neurabin-2 staining allowed us to examine the effects of blocking PirB in a larger population of neurons in the target area, rather than only in the random sample of a small number of neurons identified with Golgi-Cox impregnation.

The results of this experiment showed that there appears to be an increase in Neurabin-2 staining in the left hemisphere (PirB blocker infused) compared to the right hemisphere (PBS infused) (**Fig. 9**). The change in pixel intensities was calculated using a 5x5 grid (described above) to calculate the average pixel intensity for each square within the grid in the prelimbic area, and dividing that number by the average pixel intensity of the corresponding square in the grid within the motor cortex. These results are summarized in **Figure 10**. It should be noted that a relative ratio that exceeds 1.0 would represent that the pixel intensity was significantly elevated in the prelimbic area (where PirB blocker or PBS was infused) compared to the non-targeted region of the motor cortex. By normalizing the relative pixel intensity within each hemisphere (i.e., prelimbic area vs. motor cortex within left hemisphere) and then comparing the relative ratios between the hemispheres (**Fig. 10**), we would control for any hemispheric-specific differences in overall staining intensity. Using this approach, we can conclude that the PirB blocker had a positive global effect on the expression of the synaptic scaffolding protein Neurabin-2, which is concentrated in dendritic spines.
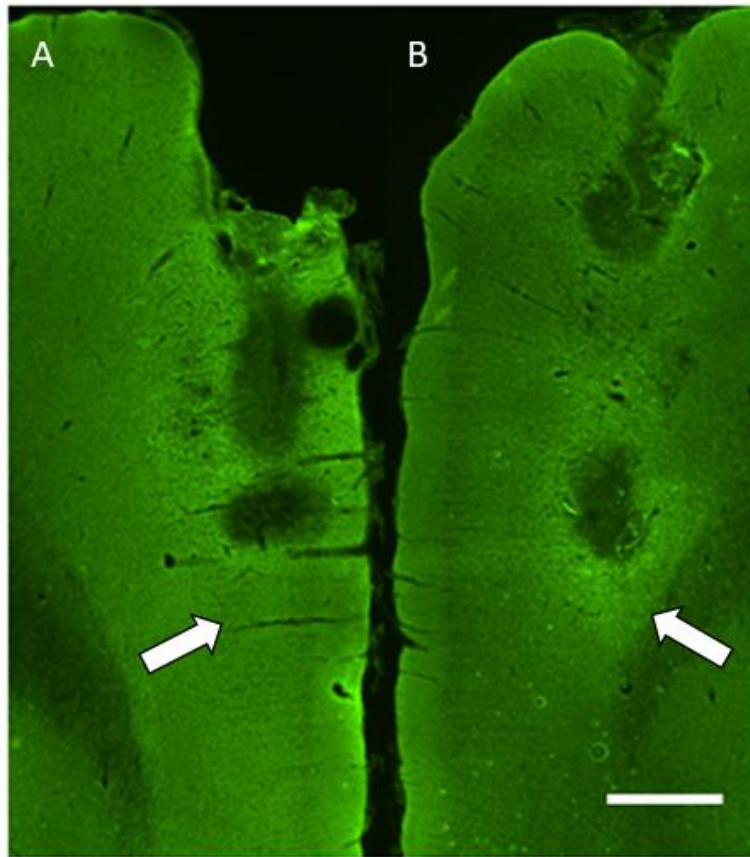
Figure 9. Immunohistochemical staining of Neurabin-2. (A) Right hemisphere (PBS infused) at 2x objective. **(B)** Left hemisphere (PirB blocker infused) at 2x objective. Scale bar represents 500 µm. Images A and B were captured using identical parameters (e.g., exposure time) for comparison. White arrow is pointing to the prelimbic area.
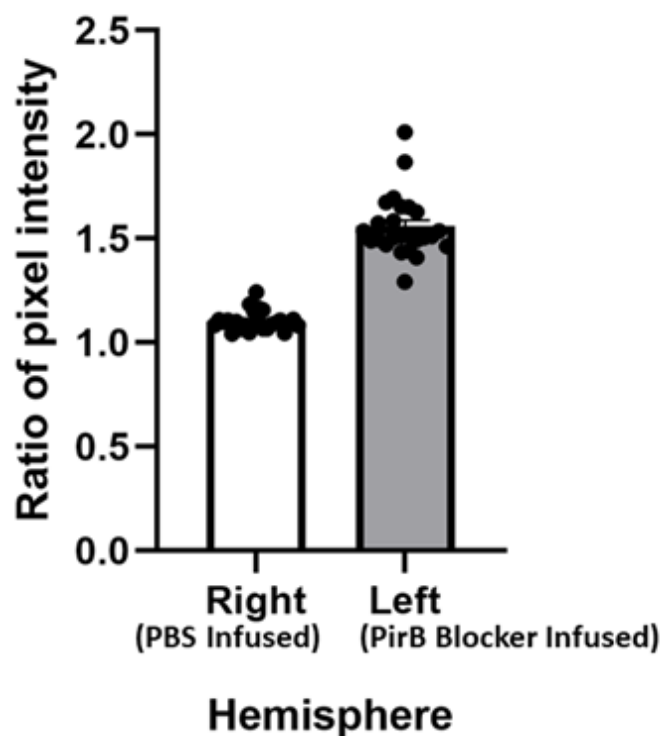
Figure 10. Ratio of pixel intensities associated with Neurabin-2 labelling in the right (PBS infused) and left (PirB blocker infused) hemispheres. The ratio of pixel intensities was calculated using a 5x5 grid in both the motor cortex and the prelimbic area in each hemisphere. The average pixel intensity of each square in the prelimbic area grid was divided by the average pixel intensity of the corresponding square in the motor cortex grid. Bars represent average ratio of pixel change for each hemisphere, circles represent individual ratios for each grid square and error bars represent SEM.

Chapter 4

4   Discussion

The overall aim of this thesis was to determine whether blocking PirB function in the prelimbic area of the mPFC would increase dendritic spine density in rats whose dendritic spine density is reduced following neonatal subplate lesions and adolescent stress. Overall, the results of this thesis suggest that blocking PirB function does indeed increase dendritic spine growth in the prelimbic area. These findings were specific to the prelimbic area, where the PirB blocker had been infused.

4.1   Confirmation of stereotaxic location of the infusion site

The first objective was to confirm that the target location had been properly cannulated in the prelimbic area. This was accomplished using a combination of stereotaxic surgery and chronic cannulae implantation, followed by rhodamine infusion and NeuroTrace counterstaining. As seen in **Figure 5**, when compared to a Rat Brain Atlas (Paxinos & Watson, 2006) and the NeuroTrace counterstain, it is clear that the rhodamine was indeed infused to the prelimbic area. These results were important because they provided confirmation that our chosen stereotaxic coordinates would ultimately allow for the PirB blocker to be subsequently infused to the target location (i.e., the prelimbic area).

4.2   Quantitative assessment of dendritic spine densities along individual dendrites in layers 2/3 using the Golgi-Cox method

The second objective of this thesis was to quantify spine densities on Golgi-Cox impregnated neurons. Golgi-Cox impregnation only labels less than 10% of neurons, allowing for imaging and analysis of full neurons and entire dendritic arbors, including dendritic spines. As such, the Golgi-Cox method allows for the full quantification of dendritic spine densities. The animal model used in the current thesis was a two-hit model, in which rats received neonatal subplate lesions (first hit), followed by adolescent stressors (second hit). Previous literature looking at dendritic spine densities in the rat mPFC have shown that on average, healthy control rats have a spine density of

approximately 1 spine per µm along basal dendrites of pyramidal neurons (Dingess et al., 2017; Leuner & Gould, 2010; Murmu et al., 2006). The current thesis showed a basal spine density of 0.69 spines per µm along the dendrites of layers 2/3 pyramidal cells in the prelimbic area of the right (PBS infused) hemisphere, which was the hemisphere that received the control infusion. This suggests that our two-hit animal model had an average reduction of 31% in the number of dendritic spines in the prelimbic area of the mPFC.

The first part of the quantification experiment in this thesis was conducted to look at spine densities outside of the prelimbic area, in M1, in order to ensure that there was no spontaneous recovery of dendritic spine density throughout the PFC. For this part of the thesis, tertiary basal dendrites just rostral and lateral to the injection site in layers 2/3 pyramidal cells were analyzed. Previous literature examining dendritic spine densities in the rat motor cortex have shown that, on average, rat motor cortical dendrites have a basal spine density of approximately 0.9 spines per µm (Adkins et al., 2002; Papadopoulos et al., 2006), which is slightly less than the approximately 1 spine per µm previously described in the mPFC. The current thesis showed a spine density of 0.64 spines per µm in the right hemisphere (PBS infused), and 0.62 spines per µm in the left hemisphere (PirB blocker infused) of M1. These results suggest that there was approximately an average reduction of 29% in the number of dendritic spines in M1. This decrease was slightly less than that observed in the prelimbic area (31% reduction), suggesting that the stress exposure reduced spine density throughout the PFC, while the early postnatal subplate lesion caused spine loss in the prelimbic area only. When looking at the variance of the spine densities measured for each animal (**Fig. 6**), our data show that no spine growth occurred in the motor cortex, while spine growth did occur in the prelimbic area following infusions of PirB blocker. This suggests that blocking PirB function in the prelimbic area does increase dendritic spine growth in the prelimbic area, but that no spontaneous growth of spines was occurring outside of the prelimbic area. Quantification of these results in M1 showed no significant difference between overall spine densities in the left and right hemispheres. These results confirmed that no spontaneous growth of dendritic spines had occurred outside of the prelimbic area following subplate lesioning and adolescent stress, which suggests that any changes

(increases) observed within the prelimbic area are indeed due to the administration of PirB blocker itself (**Fig. 7**).

Consistent with our hypothesis, the results of the Golgi-Cox impregnated neurons suggest that when PirB is infused to the prelimbic area, dendritic spine density was significantly increased compared to the side that received a vehicle (PBS) infusion (**Fig. 8**). Consistent with previous studies in which PirB blocker was administered to other brain regions (e.g., the visual cortex), it appears that, under normal conditions, the presence of PirB in the mPFC causes decreased dendritic spine growth in the adult brain (Bochner et al., 2017; Djurisic et al., 2013). In the current thesis, treatment with PirB blocker in the prelimbic area of the left hemisphere increased dendritic spine density to 0.99 spines per µm, indicating that blocking PirB in the prelimbic area rescued spine loss to levels of spines typically seen in the mPFC of healthy, control rats (Dingess et al., 2017; Leuner & Gould, 2010; Murmu et al., 2006). These are particularly exciting findings as it appears that blocking PirB was fully capable of counter-acting the ~31% average reduction in spine density caused by the two-hit model of neonatal subplate lesion and adolescent stress.

In comparing the effects observed in past studies, the results of the current thesis showed an average increase of 44% (i.e., 0.99 spines per µm in the left hemisphere vs. 0.69 spines per µm in the right hemisphere) in dendritic spine density following PirB blocker infusions, whereas in the visual cortex of PirB-/- mice, the increase in spine density was ~175% compared to wildtype mice (Djurisic et al., 2013), and in the visual cortex of mice that had received infusions of PirB blocker the increase was 57% (Bochner et al., 2017). It makes sense that the knockout mice would have a greater relative increase in spine density compared to rodents that received PirB blocker infusions, as the PirB-/- mice had no PirB at all, and thus, they would have never had the inhibition of spine growth associated with PirB function in the adult brain. In contrast, rodents that received infusions of PirB blocker still had PirB throughout their brain, thus allowing for the activity of PirB to inhibit spine growth throughout the lifespan. It is worth noting that the difference in the relative degree to which dendritic spine growth occurred following PirB blocker infusions in the mPFC (current thesis) versus the visual cortex (57%; Bochner et

al., 2017) could be explained by a few different factors. First, it is possible that dendritic spine density is differentially regulated in the mPFC compared to the visual cortex. The mPFC is a multi-sensory brain region, whereas the visual cortex is a primary sensory brain region, and the differential organization of these two brain regions could have an effect on how they respond to the PirB blocker treatment. For example, it has been shown that pyramidal neurons in the human PFC contain up to 23x more dendritic spines than pyramidal cells of the visual cortex (Elston et al., 2003), and while studies have shown the overall spread of PirB expression across the cerebral cortex, hippocampus and cerebellum (Mi et al., 2017), no comparison has been made between expression levels of PirB within the cerebral cortex (i.e., between the visual cortex and the PFC). It is possible that the amount of PirB present within the PFC is higher than in the visual cortex, meaning that more PirB blocker would be required to achieve the same level of new spine growth. To test this, Western blotting for PirB could be conducted in both brain regions to determine the relative expression levels of the receptor and how they compare to one another. In addition to differences between the visual cortex and PFC, the differences observed between the relative increase in spine density in the current thesis compared to previous literature could be explained by the different infusion protocols used. Bochner et al., (2017) used an infusion protocol in which PirB blocker was infused to the visual cortex for 11 days, whereas the current thesis infused PirB blocker for 5 days. The present choice to use a shorter duration infusion protocol was based on an effort to preserve the integrity of the implanted guide cannulae, which can become loose in the skull after 2-3 weeks of chronic implantation. Importantly, despite the shorter duration infusion protocol, the current thesis has confirmed that infusing PirB blocker twice per day for 5 days is sufficient to cause a significant (44%) increase in dendritic spine density. That said, further experimental studies (described in section 4.6) should be conducted using the current 5-day infusion protocol to determine if a 44% increase in dendritic spines is sufficient to cause behavioral changes. If no behavioral changes were to occur following 5 days of PirB blocker infusions, it would be worth-while to infuse the PirB blocker for a longer period of time, as was done by Bochner et al., (2017). Finally, it should be noted that although the relative increase in spine density was less in the mPFC

than in the visual cortex, the 44% spine increase was still sufficient to return spine density to normal levels as per the previous literature (discussed above).

4.3 Assessment of the global effect of blocking PirB in the mPFC using immunohistochemistry

The third objective of this thesis was to gain a better understanding of the effect of blocking PirB function on dendritic spine density on a global level. Given that Golgi-Cox impregnation only labels less than 10% of all neurons, in order to ensure that the obtained results were not limited to the small sample of randomly stained neurons, immunohistochemical labelling of the synaptic scaffolding protein Neurabin-2 was conducted and the differences between the right and left hemispheres were qualitatively assessed. As seen in **Figure 9**, there appeared to be more fluorescent staining of Neurabin-2 in the left hemisphere (PirB blocker infused) compared to the right hemisphere (PBS infused), meaning that there was more of the synaptic scaffolding protein present when PirB function was blocked. Neurabin-2 has been shown to be concentrated in dendritic spines and can therefore be used as an indirect marker of spine density (Satoh et al., 1998). Quantification of the pixel intensity ratios showed that upon PirB blocking, there appeared to be a difference between the pixel intensity change in the motor cortex (used as a control) and the prelimbic area. More specifically, the left hemisphere appeared to have a larger pixel intensity change ratio compared to the right hemisphere, suggesting that there were more dendritic spines present following administration of PirB blocker into the left hemisphere (**Fig. 10**). Importantly, these immunohistochemical findings are consistent with the Golgi-Cox impregnation results, and suggest that blocking PirB function in the prelimbic area increased spine density on a global scale and not only on the randomly labelled neurons observed with the Golgi-Cox method.

Due to the known role of the PFC in executive function, understanding the mechanisms that regulate its growth/loss of dendritic spines could be incredibly useful for disorders that affect higher-cognitive function. For example, patients with schizophrenia have a decreased gray matter volume largely due to a loss of dendritic spines in the dlPFC (Glantz & Lewis, 2000) and in turn, deficits in multiple areas of cognition (Gold, 2004).

In particular, patients with schizophrenia have difficulty with executive function, which causes many challenges in everyday life (Everett et al., 2001; Haut et al., 1996; Koren et al., 1998; Li, 2004). Normal executive function is required to inhibit unwanted actions and be mentally flexible, and patients with deficits in these areas have devastating outcomes in everyday life. In the lab, patients with schizophrenia have difficulties performing tasks of executive function such as the Wisconsin Card Sorting Task. Overall, the experiments in this thesis have helped to improve our understanding as to how dendritic spine growth is regulated and inhibited in the PFC, and how that inhibition can be arrested in order to allow for the growth of new dendritic spines.

4.4 Implications

Looking beyond the neuroanatomical confirmation that PirB controls dendritic spine growth, the results of the current thesis provide a promising first step in the development of a novel treatment for the cognitive deficits in schizophrenia. The cognitive deficits of schizophrenia include impairments in attention, working memory and executive function; a constellation of deficits that have been shown to be associated with a decreased gray matter volume in the dlPFC (Rüsch et al., 2007). This decrease in gray matter volume is the result of a marked reduction in the number of dendritic spines on layer 3 pyramidal cells in the dlPFC (Glantz & Lewis, 2000). Excitingly, using a rodent model with features consistent with schizophrenia, the experiments in the current thesis have shown that blocking the function of the immune receptor PirB in the prelimbic area significantly increased the dendritic spine densities on layers 2/3 pyramidal cells. In the human brain, there is an ortholog of PirB called human leukocyte immunoglobulin-like receptor B2 (LILB2) (Atwal et al., 2008). By extension, the presence of a human ortholog provides the possibility of eventually applying our preclinical findings to human schizophrenia patients with the goal of growing dendritic spines in an attempt to alleviate their cognitive deficits. Ultimately, if spine densities in the dlPFC of schizophrenia patients can be increased, it is possible that the commonly observed deficits in executive function, working memory and attention may be at least partially recovered. In fact, if these deficits could be alleviated through a novel therapeutic approach such as blocking PirB function, schizophrenia patients would then have access to treatments to help offset their

positive, negative, and cognitive symptoms. Given that the cognitive deficits in schizophrenia are devastating and prevent many patients from living ordinary lives, there remains an unmet clinical need to design, test and validate putative therapeutic approaches.

The implications of this research are not limited to schizophrenia. As previously discussed, many neurological disorders are associated with a decreased dendritic spine density in different brain regions. The cognitive impairments in Alzheimer's Disease have been shown to be associated with a decreased dendritic spine density in the hippocampus (DeKosky & Scheff, 1990; Terry et al., 1991). Additionally, the motor deficits seen in Parkinson's Disease are thought to be caused by dendritic spine loss in medium spiny neurons in the caudal putamen and the caudate nucleus (MacNeill et al., 1988; Stephens et al., 2005; Zaja-Miltatovic et al., 2005). Patients with bipolar disorder have also been shown to have a lower dendritic spine density in the dlPFC compared to healthy controls (Konopaske et al., 2014). Finally, dendritic spine loss has been observed in multiple brain regions of patients and animals suffering from depression, anxiety and chronic stress (Goldwater et al., 2009; Kang et al., 2012; Kassem et al., 2013; Radley et al., 2006; Soetanto et al., 2010; Welch et al., 2007). As dendritic spine loss is a common issue in many different neurological disorders, concerted efforts to effectively increase the density of dendritic spines in different brain regions could help to alleviate the associated symptoms. To date, blocking PirB function has now been shown to increase dendritic spine density in the visual cortex (Bochner et al., 2017; Djurisic et al., 2013) and the mPFC (current thesis). Thus, future research should be conducted in order to determine the effects of blocking PirB function in other brain regions associated with dendritic spine loss and neurological disorders.

4.5   Experimental challenges and limitations

Unfortunately, restrictions due to the COVID-19 pandemic meant that new animals were unable to be ordered over the summer of 2020. This delay in animal ordering meant that we were unable to perform the planned behavioral experiments (described in detail in the 'Future Directions' section), which sought to complement our neuroanatomical investigation (described in current thesis) and provide a complete picture of the

functionality and maturity of the newly formed dendritic spines. These behavioral experiments should be conducted in the future.

In addition to the pandemic, time was a limitation in terms of the Golgi-Cox method. The staining procedure followed the protocol described by Zaqout & Kaindl, 2016; however, multiple caveats had to be overcome. Firstly, background staining of myelin was an issue at first, as the current study used adult rats. Adult brains contain more myelin than young brains, which generate background staining and can take away from the neuronal labelling. Over the span of approximately four months, we were able to reduce the background staining of myelin to the point in which mainly neurons were stained, and spines were able to be analyzed. Another issue that arose while attempting the Golgi-Cox method was slicing the brains. The brains were unfixed to allow for proper impregnation of the Golgi-Cox solution; however, slicing unfixed brain tissue is not ideal. It took several more months of attempting to slice on different machines (i.e., microtome, cryostat) with different thicknesses until we could successfully slice our 200 µm thick slices on the vibratome. The process of making a new Golgi-Cox impregnation protocol appropriate for adult rat brains took approximately 6 months, and if the protocol had of been in place prior, that time could have been used to take animals through behavioral testing. Thankfully, we have overcome these initial challenges, and have now developed a protocol for the Golgi-Cox method in the lab that can be used for future experiments.

Another limitation to the current thesis was the lack of inter-rater reliability, which refers to the degree to which two or more examiners agree on an experimental result. This ensures that the obtained results are not biased by the experimenter, as multiple examiners would be required to come to the same conclusion in order for the results to have a high inter-rater reliability. In future studies conducted to further the work of the current thesis, images should be taken and spine densities should be analyzed by one examiner, then given to a second examiner to analyze. In addition to having a second examiner analyze spine densities, this second examiner could be blinded to the experimental condition of the dendrites being analyzed. This would further ensure that the results are free from bias, and that the changes in spine density were truly due to blocking PirB in the mPFC.

A final limitation to the current thesis was that only a small number of dendrites were available for analysis for each animal. Due to the nature of Golgi-Cox impregnation in which only less than 10% of all neurons are stained, as well as the specific dendrites of interest (i.e., tertiary layers 2/3 basal pyramidal neurons), only a fairly small number of dendrites meeting all criteria were present. This limitation was partially alleviated by the use of immunohistochemical labelling of Neurabin-2 to gain an overall global view of the effects of blocking PirB function in the prelimbic area; however, if more dendrites had of been available for analysis in the Golgi-Cox impregnation experiment, the statistical analysis would have had more power. This could be addressed in future experiments by taking more animals through the entire procedure, thus increasing the sample size.

4.6 Future directions

The results of this thesis provide the basis for many future studies. Here, we have shown that blocking PirB in the prelimbic area allows for growth of new dendritic spines. Next, it will be crucial to determine whether these newly formed dendritic spines are functional. In order to answer this question, electrophysiological and behavioral studies should be conducted. The electrophysiological properties of these newly formed spines should be measured in order to quantify their overall function. This should be followed by studies to determine establishment of appropriate synaptic connections on the newly formed dendritic spines, and finally, behavioral studies should be conducted in order to observe whether or not functional deficits in schizophrenia can be ameliorated by growing new dendritic spines on layers 2/3 pyramidal cells in the prelimbic area of the mPFC.

The electrophysiological properties of dendritic spines can be quantified by measuring miniature post-synaptic potentials (mEPSPs), which are generated by the spontaneous release of neurotransmitters from a presynaptic axon terminal in the absence of an action potential (Fatt & Katz, 1952). mEPSPs are thought to represent the quantal release of one single vesicle of neurotransmitter (Streit & Lüscher, 1991). In particular, mEPSPs can be used to quantify the baseline activity of excitatory synapses in the absence of presynaptic action potentials. mEPSPs can be measured using whole-cell patch clamping and quantified in terms of both amplitude and frequency. The frequency of mEPSPs is used to determine changes in the number of functional excitatory synapses. In order to determine

whether the newly formed dendritic spines in the current thesis are functional, whole-cell patch-clamping should be conducted following infusions of the PirB blocker and vehicle, and mEPSP frequencies should be compared between the two hemispheres. If the new spines are functional, it would be predicted that there would be an increase in the frequency but not the amplitude of mEPSPs in the hemisphere that had received the PirB blocker compared to the hemisphere that had received vehicle infusions.

In addition to electrophysiological studies, double labelling immunohistochemistry should be conducted in order to determine whether these newly grown dendritic spines have formed appropriate synapses with presynaptic terminals. This can be achieved by immunohistochemical labelling of both Neurabin-2 (concentrated in dendritic spines) and a presynaptic marker such as VGlutT2 (concentrated in presynaptic terminals). Sections from the mPFC of animals that received infusions of PirB blocker, as in the present study, would be double immunolabeled using these antibodies raised in different species and the positive labelling would be identified using secondary antibodies conjugated to different color (e.g., red and green) fluorochromes. This would allow us to determine whether new dendritic spines grown following pharmacological blocking of PirB in the mPFC are forming synapses and participating in appropriate synaptic circuitry.

Finally, it is crucial to determine the effects of blocking PirB function in the prelimbic area on cognitive function. In particular, given that executive function is impaired in schizophrenia and is associated with a decreased dendritic spine density on layers 2/3 pyramidal cells in the prelimbic area, it would be expected that when PirB function is blocked and dendritic spine density is increased in the prelimbic area, executive function would improve as well. The original plan for the current thesis was to test executive function following infusions of the PirB blocker; however, as described in the limitations section, due to the COVID-19 pandemic and restrictions around ordering new animals during the lockdowns, behavioral testing was unable to occur as part of this thesis. If cognitive testing were to have been conducted according to the original plan, behavioral set-shifting would have been performed to test changes in executive function after blocking PirB function in the prelimbic area of both hemispheres. Behavioral set-shifting is a task that tests executive function and relies heavily on the PFC. In the set-shifting

task, there are two main phases, which can be followed by a reversal learning task (another form of cognitive flexibility). Set-shifting and reversal learning can be performed by placing food-restricted rats inside a sound-attenuated behavior box with two levers (on the left and right side of the box), two lights (one just above each lever), and a feeding trough between the two levers connected to a sugar pellet dispenser. The first phase of the set-shifting task is called Visual Cue Discrimination. In this phase, animals are required to learn to press a lever that is associated with a light. For each trial, the left and right levers are presented to the animal at the same time, and one of the two lights is randomly illuminated. Each time the animal correctly presses the lever on the same side as the light, a sugar pellet is dispensed into the food trough. This continues for a total of 100 trials, and performance can be scored by the number of total errors made. The day after the animal has learned the Visual Cue Discrimination rule, they are placed back inside the behavior box and must repeat this task for 20 trials to test their memory of the visual cue rule (i.e., the first "set"). On the 21st trial, the rule switches and the second phase of the set-shifting task begins. This phase of the set-shifting task is called Response Discrimination. Now, animals must ignore the visual cue and instead press the lever on only one side (e.g., only the left lever). Ultimately, in order to learn this new rule and demonstrate set-shifting ability, the rats must unlearn the original rule of following the light, and adopt the new side-based rule. The Response Discrimination task is repeated for 120 trials, and performance can be scored by the number of errors made. Once again, the rats are tested for memory retention on 20 trials the following day. Finally, if there is the desire to now test the rat's ability for reversal learning, on the 21st trial, the rule switches once again, and now requires the rat to press the lever on the opposite side to the Response Discrimination day (i.e., only the right lever). The two phases of the set-shifting task are summarized in **Figure 11** (note: reversal learning is not shown).

The ability to set-shift has been shown to rely on function of the mPFC (Birrell & Brown, 2000; Floresco et al., 2008), whereas reversal learning has been shown to involve the orbitofrontal cortex (Ghods-Sharifi et al., 2008). Overall, a rat's set-shifting ability can be measured by quantifying three main error types; perseverative, regressive and never reinforced. Perseverative errors occur when the rat has difficulties ignoring the previously learned rule and thus perseveres with the original rule. This error type has been shown to

increase when dopaminergic circuitry between the medial dorsal thalamus and the mPFC is disrupted (Block et al., 2007; Floresco et al., 2006). Regressive errors refer to errors made in maintaining the newly learned rule, and have been shown to involve the nucleus accumbens core and dorsomedial striatum (Floresco et al., 2006). Recall that humans with schizophrenia have been shown to make more perseverative errors compared to healthy controls on tasks like this set-shifting task in rodents (e.g., Wisconsin Card Sorting Task) Everett et al., 2001; Haut et al., 1996; Koren et al., 1998; Li, 2004).

Prior to the COVID-19 lockdowns, I was able to train a cohort of animals and conduct the entire set-shifting protocol for a study conducted in our lab by Wieczerzak et al., 2021. The results of this behavioral testing are shown in **Appendix A**, demonstrating that had I been able to order new animals in time during the lockdown, I would have been prepared to run the two-hit rats through an identical protocol following PirB blocker infusions. As a previous study in our lab has shown that NGF infusions into the neonatal frontal cortex (i.e., the subplate lesion model) causes adult rats to make more perseverative errors on the set-shifting task compared to sham lesioned rats (Desai et al., 2018), it was predicted that increasing dendritic spine density on layers 2/3 pyramidal cells in the prelimbic area of these rats would improve cognitive flexibility. In considering the possible extent that executive function could be rescued in our two-hit model, Bochner et al., 2017 showed that in the visual cortex, blocking PirB increases dendritic spine density to normal levels; however, visual acuity was only partially recovered. Based on these results, it would be reasonable to predict that blocking PirB function in the prelimbic area could decrease the number of perseverative errors made on the set-shifting task but perhaps not quite to normal levels. Overall, further research is required in order to conclude whether the newly formed dendritic spines observed in the current thesis would ultimately lead to functional recovery of executive function.
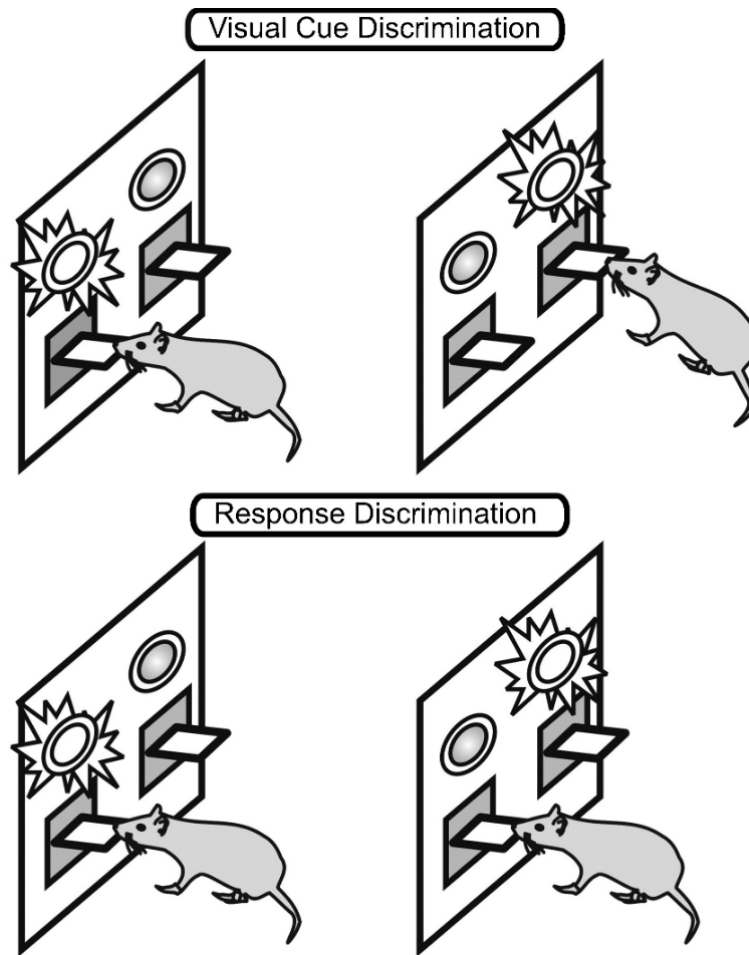
Figure 11. Overview of behavioral set-shifting task. Visual Cue Discrimination requires animals to learn to press a lever associated with a light. Response Discrimination requires animals to unlearn the originally-learned rule, ignore the light, and press the lever on one side only (e.g., the left lever). (Image adapted from Floresco et al., 2008).

4.7   Conclusions

The results of the current thesis provide a promising step towards developing a successful novel treatment for the cognitive deficits of schizophrenia, which can have devastating effects on the quality of life of patients suffering with this psychiatric disorder. For example, patients with schizophrenia have a difficult time with behavioral flexibility, a form of executive function that relies heavily on the dlPFC, which has been shown to have a reduced number of dendritic spines in schizophrenia. These results provide a potential target for growing new dendritic spines in this brain region in patients with schizophrenia in an attempt to alleviate some of the cognitive symptoms associated with this disease. The preclinical experiments conducted in this thesis may also have implications for many neurological disorders with disrupted cortical neurotransmission such as Alzheimer's Disease, Huntington's Disease, etc. Developing a method for improving cognition by allowing for neural plasticity to occur past the critical period could open the door to a new set of experimental procedures for looking at different neurological disorders.

In the future, electrophysiological tests should be conducted in order to determine the functionality of these newly formed dendritic spines by measuring the frequency of spontaneous mEPSPs (described above). In addition to electrophysiological testing, behavioral tests of executive function (i.e., set-shifting) will be a crucial next step in determining whether the increased dendritic spine density observed here translates to an increase in performance on these translational behavioral tasks. This will provide us with further insight into the effectiveness of this potential treatment for the cognitive deficits of schizophrenia. Furthermore, it will be crucial to investigate all other areas of the brain that express PirB and see how blocking its activity affects other aspects of behavior.

Overall, the results of this thesis are very exciting and will lead the way for many future experiments. We have shown for the first time that blocking PirB function in the mPFC increases dendritic spine density, providing new insight into how spine growth is regulated in adulthood in the mPFC. If the newly formed spines are functional, this preclinical research could help lead toward the potential development of a new treatment

for the cognitive deficits in schizophrenia, as well as deficits involving spine loss in other brain regions.

References

Abbott, M. A., Wells, D. G., & Fallon, J. R. (1999). The insulin receptor tyrosine kinase substrate p58/53 and the insulin receptor are components of CNS synapses. *Journal of Neuroscience*, *19*(17), 7300-7308.

Adkins, D. L., Bury, S. D., & Jones, T. A. (2002). Laminar-dependent dendritic spine alterations in the motor cortex of adult rats following callosal transection and forced forelimb use. *Neurobiology of learning and memory*, *78*(1), 35-52.

Akulinin, V. A., Stepanov, S. S., Semchenko, V. V., & Belichenko, P. V. (1997). Dendritic changes of the pyramidal neurons in layer V of sensory-motor cortex of the rat brain during the postresuscitation period. *Resuscitation*, *35*(2), 157-164.

Anticevic, A., Cole, M. W., Repovs, G., Murray, J. D., Brumbaugh, M. S., Winkler, A. M., Savic, A., Krystal, J. H., Pearlson, G. D., & Glahn, D. C. (2014). Characterizing thalamo-cortical disturbances in schizophrenia and bipolar illness. *Cerebral cortex*, *24*(12), 3116-3130.

Arnsten, A. F. T., & Manji, H. K. (2008). Mania: a rational neurobiology.

Atwal, J. K., Pinkston-Gosse, J., Syken, J., Stawicki, S., Wu, Y., Shatz, C., & Tessier-Lavigne, M. (2008). PirB is a functional receptor for myelin inhibitors of axonal regeneration. *Science*, *322*(5903), 967-970.

Baum, A. E., Akula, N., Cabanero, M., Cardona, I., Corona, W., Klemens, B., Schulze, T. G., Cichon, S., Rietschel, M., Nöthen, M. M., Georgi, A., & McMahon, F. J. (2008). A genome-wide association study implicates diacylglycerol kinase eta (DGKH) and several other genes in the etiology of bipolar disorder. *Molecular psychiatry*, *13*(2), 197-207.

Benavides-Piccione, R., Fernaud-Espinosa, I., Robles, V., Yuste, R., & DeFelipe, J. (2013). Age-based comparison of human dendritic spine structure using complete three-dimensional reconstructions. *Cerebral cortex*, *23*(8), 1798-1810.

Blanchoin, L., Boujemaa-Paterski, R., Sykes, C., & Plastino, J. (2014). Actin dynamics, architecture, and mechanics in cell motility. *Physiological reviews*, *94*(1), 235-263.

Block, A. E., Dhanji, H., Thompson-Tardif, S. F., & Floresco, S. B. (2007). Thalamic–prefrontal cortical–ventral striatal circuitry mediates dissociable components of strategy set shifting. *Cerebral cortex*, *17*(7), 1625-1636.

Bloss, E. B., Janssen, W. G., Ohm, D. T., Yuk, F. J., Wadsworth, S., Saardi, K. M., McEwen, B. S., & Morrison, J. H. (2011). Evidence for reduced experience-dependent dendritic spine plasticity in the aging prefrontal cortex. *Journal of Neuroscience*, *31*(21), 7831-7839.

Bocarsly, M. E., Fasolino, M., Kane, G. A., LaMarca, E. A., Kirschen, G. W., Karatsoreos, I. N., McEwen, B. S., & Gould, E. (2015). Obesity diminishes synaptic markers, alters microglial morphology, and impairs cognitive function. *Proceedings of the National Academy of Sciences*, *112*(51), 15731-15736.

Bochner, D. N., Sapp, R. W., Adelson, J. D., Zhang, S., Lee, H., Djurisic, M., Syken, J., Dan, Y., & Shatz, C. J. (2014). Blocking PirB up-regulates spines and functional synapses to unlock visual cortical plasticity and facilitate recovery from amblyopia. *Science translational medicine*, *6*(258), 258ra140-258ra140.

Broberg, B. V., Dias, R., Glenthøj, B. Y., & Olsen, C. K. (2008). Evaluation of a neurodevelopmental model of schizophrenia—early postnatal PCP treatment in attentional set-shifting. *Behavioural brain research*, *190*(1), 160-163.

Brodbeck, J., Balestra, M. E., Saunders, A. M., Roses, A. D., Mahley, R. W., & Huang, Y. (2008). Rosiglitazone increases dendritic spine density and rescues spine loss caused by apolipoprotein E4 in primary cortical neurons. *Proceedings of the National Academy of Sciences*, *105*(4), 1343-1346.

Calabrese, B., & Halpain, S. (2005). Essential role for the PKC target MARCKS in maintaining dendritic spine morphology. *Neuron*, *48*(1), 77-90.

Choi, J., Ko, J., Racz, B., Burette, A., Lee, J. R., Kim, S., Na, M., Lee, H. W., Kim, K., Weinberg, R. J., & Kim, E. (2005). Regulation of dendritic spine morphogenesis by insulin receptor substrate 53, a downstream effector of Rac1 and Cdc42 small GTPases. *Journal of Neuroscience*, *25*(4), 869-879.

Chung, W., Choi, S. Y., Lee, E., Park, H., Kang, J., Park, H., Choi, Y., Lee, D., Park, S., Kim, R., Cho, Y. S., Choi, J., Kim, M., Lee, J. W., Lee, S., Rhim, I., Jung, M. W., Kim, D., Bae, Y. C., & Kim, E. (2015). Social deficits in IRSp53 mutant mice improved by NMDAR and mGluR5 suppression. *Nature neuroscience*, *18*(3), 435-443.

Craft, S., Dagogo-Jack, S. E., Wiethop, B. V., Murphy, C., Nevins, R. T., Fleischman, S., Rice, S., Newcomer, V., John, W., Cryer, P. E., (1993). Effects of hyperglycemia on memory and hormone levels in dementia of the Alzheimer type: a longitudinal study. *Behavioral neuroscience*, *107*(6), 926.

Day, M., Wang, Z., Ding, J., An, X., Ingham, C. A., Shering, A. F., Wokosin, D., Ilijic, E., Sun, Z., Sampson, A. R., Mugnaini, E., Deutch, A. Y., Sesack, S. R., Arbuthnott, G. W., & Surmeier, D. J. (2006). Selective elimination of glutamatergic synapses on striatopallidal neurons in Parkinson disease models. *Nature neuroscience*, *9*(2), 251-259.

Day, C. (1999). Thiazolidinediones: a new class of antidiabetic drugs. *Diabetic Medicine*, *16*(3), 179-192.

DeKosky, S. T., & Scheff, S. W. (1990). Synapse loss in frontal cortex biopsies in Alzheimer's disease: correlation with cognitive severity. *Annals of Neurology: Official Journal of the American Neurological Association and the Child Neurology Society*, *27*(5), 457-464.

Desai, S. J., Allman, B. L., & Rajakumar, N. (2018). Infusions of nerve growth factor into the developing frontal cortex leads to deficits in behavioral flexibility and increased perseverance. *Schizophrenia bulletin*, *44*(5), 1081-1090.

Desmond, N. L., & Levy, W. B. (1986). Changes in the numerical density of synaptic contacts with long-term potentiation in the hippocampal dentate gyrus. *Journal of Comparative Neurology*, *253*(4), 466-475.

Deutch, A. Y., Colbran, R. J., & Winder, D. J. (2007). Striatal plasticity and medium spiny neuron dendritic remodeling in parkinsonism. *Parkinsonism & related disorders*, *13*, S251-S258.

Dingess, P. M., Darling, R. A., Dolence, E. K., Culver, B. W., & Brown, T. E. (2017). Exposure to a diet high in fat attenuates dendritic spine density in the medial prefrontal cortex. *Brain Structure and Function*, *222*(2), 1077-1085.

Djurisic, M., Vidal, G. S., Mann, M., Aharon, A., Kim, T., Santos, A. F., Zuo, Y., Hübener, M., & Shatz, C. J. (2013). PirB regulates a structural substrate for cortical plasticity. *Proceedings of the National Academy of Sciences*, *110*(51), 20771-20776.

Dos Remedios, C. G., Chhabra, D., Kekic, M., Dedova, I. V., Tsubakihara, M., Berry, D. A., & Nosworthy, N. J. (2003). Actin binding proteins: regulation of cytoskeletal microfilaments. *Physiological reviews*, *83*(2), 433-473.

Dumitriu, D., Hao, J., Hara, Y., Kaufmann, J., Janssen, W. G., Lou, W., Rapp, P. R., & Morrison, J. H. (2010). Selective changes in thin spine density and morphology in monkey prefrontal cortex correlate with aging-related cognitive impairment. *Journal of Neuroscience*, *30*(22), 7507-7515.

Ellison-Wright, I., & Bullmore, E. (2010). Anatomy of bipolar disorder and schizophrenia: a meta-analysis. *Schizophrenia research*, *117*(1), 1-12.

Elston, G. N. (2003). Cortex, cognition and the cell: new insights into the pyramidal neuron and prefrontal function. *Cerebral cortex*, *13*(11), 1124-1138.

Engert, F., & Bonhoeffer, T. (1999). Dendritic spine changes associated with hippocampal long-term synaptic plasticity. *Nature*, *399*(6731), 66-70.

Everett, J., Lavoie, K., Gagnon, J. F., & Gosselin, N. (2001). Performance of patients with schizophrenia on the Wisconsin Card Sorting Test (WCST). *Journal of Psychiatry and Neuroscience*, *26*(2), 123.

Fatt, P., & Katz, B. (1952). Spontaneous subthreshold activity at motor nerve endings. *The Journal of physiology*, *117*(1), 109.

Feinstein, D. L., Spagnolo, A., Akar, C., Weinberg, G., Murphy, P., Gavrilyuk, V., & Russo, C. D. (2005). Receptor-independent actions of PPAR thiazolidinedione agonists: is mitochondrial function the key?. *Biochemical pharmacology*, *70*(2), 177-188.

Fifková, E., & Anderson, C. L. (1981). Stimulation-induced changes in dimensions of stalks of dendritic spines in the dentate molecular layer. *Experimental neurology*, *74*(2), 621-627.

Flagstad, P., Glenthøj, B. Y., & Didriksen, M. (2005). Cognitive deficits caused by late gestational disruption of neurogenesis in rats: a preclinical model of schizophrenia. *Neuropsychopharmacology*, *30*(2), 250-260.

Floresco, S. B., Block, A. E., & Maric, T. L. (2008). Inactivation of the medial prefrontal cortex of the rat impairs strategy set-shifting, but not reversal learning, using a novel, automated procedure. *Behavioural brain research*, *190*(1), 85-96.

Floresco, S. B., Ghods-Sharifi, S., Vexelman, C., & Magyar, O. (2006). Dissociable roles for the nucleus accumbens core and shell in regulating set shifting. *Journal of Neuroscience*, *26*(9), 2449-2457.

Fornito, A., Yücel, M., Patti, J., Wood, S. J., & Pantelis, C. (2009). Mapping grey matter reductions in schizophrenia: an anatomical likelihood estimation analysis of voxel-based morphometry studies. *Schizophrenia research*, *108*(1-3), 104-113.

Garcia, B. G., Neely, M. D., & Deutch, A. Y. (2010). Cortical regulation of striatal medium spiny neuron dendritic remodeling in parkinsonism: Modulation of glutamate release reverses dopamine depletion–induced dendritic spine loss. *Cerebral Cortex*, *20*(10), 2423-2432.

Garey, L. J., Ong, W. Y., Patel, T. S., Kanani, M., Davis, A., Mortimer, A. M., Barnes, T.R.E., & Hirsch, S. R. (1998). Reduced dendritic spine density on cerebral cortical pyramidal neurons in schizophrenia. *Journal of Neurology, Neurosurgery & Psychiatry*, *65*(4), 446-453.

Ghods-Sharifi, S., Haluk, D. M., & Floresco, S. B. (2008). Differential effects of inactivation of the orbitofrontal cortex on strategy set-shifting and reversal learning. *Neurobiology of learning and memory*, *89*(4), 567-573.

Giraldo-Chica, M., Rogers, B. P., Damon, S. M., Landman, B. A., & Woodward, N. D. (2018). Prefrontal-thalamic anatomical connectivity and executive cognitive function in schizophrenia. *Biological psychiatry*, *83*(6), 509-517.

Glahn, D. C., Laird, A. R., Ellison-Wright, I., Thelen, S. M., Robinson, J. L., Lancaster, J. L., Bullmore, E., & Fox, P. T. (2008). Meta-analysis of gray matter anomalies in schizophrenia: application of anatomic likelihood estimation and network analysis. *Biological psychiatry*, *64*(9), 774-781.

Glantz, L. A., & Lewis, D. A. (2000). Decreased dendritic spine density on prefrontal cortical pyramidal neurons in schizophrenia. *Archives of general psychiatry*, *57*(1), 65-73.

Gogtay, N., Vyas, N. S., Testa, R., Wood, S. J., & Pantelis, C. (2011). Age of onset of schizophrenia: perspectives from structural neuroimaging studies. *Schizophrenia bulletin*, *37*(3), 504-513.

Gold, J. M. (2004). Cognitive deficits as treatment targets in schizophrenia. *Schizophrenia research*, *72*(1), 21-28.

Goldwater, D. S., Pavlides, C., Hunter, R. G., Bloss, E. B., Hof, P. R., McEwen, B. S., & Morrison, J. H. (2009). Structural and functional alterations to rat medial prefrontal cortex following chronic restraint stress and recovery. *Neuroscience*, *164*(2), 798-808.

Hains, A. B., Vu, M. A. T., Maciejewski, P. K., van Dyck, C. H., Gottron, M., & Arnsten, A. F. (2009). Inhibition of protein kinase C signaling protects prefrontal cortex

dendritic spines and cognition from the effects of chronic stress. *Proceedings of the National Academy of Sciences*, *106*(42), 17957-17962.

Hajszan, T., MacLusky, N. J., & Leranth, C. (2005). Short-term treatment with the antidepressant fluoxetine triggers pyramidal dendritic spine synapse formation in rat hippocampus. *European Journal of Neuroscience, 21*(5), 1299-1303.

Harris, K. M. (1999). Structure, development, and plasticity of dendritic spines. *Current opinion in neurobiology*, *9*(3), 343-348.*Neuroscience*, *21*(5), 1299-1303.

Haut, M. W., Cahill, J., Cutlip, W. D., Stevenson, J. M., Makela, E. H., & Bloomfield, S. M. (1996). On the nature of Wisconsin Card Sorting Test performance in schizophrenia. *Psychiatry research*, *65*(1), 15-22.

Hayashi-Takagi, A., Takaki, M., Graziane, N., Seshadri, S., Murdoch, H., Dunlop, A. J., Makino, Y., Seshadri, A. J., Ishizuka, K., Srivastava, D. P., Xie, Z., Baraban, J. M., Houslay, M. D., Tomoda, T., Brandon, N. J., Kamiya, A., Yan, Z., Penzes, P., & Sawa, A. (2010). Disrupted-in-Schizophrenia 1 (DISC1) regulates spines of the glutamate synapse via Rac1. *Nature neuroscience*, *13*(3), 327.

Hayashi-Takagi, A., Araki, Y., Nakamura, M., Vollrath, B., Duron, S. G., Yan, Z., Kasai, H., Huganir, R. L., Campbell, D. A., & Sawa, A. (2014). PAKs inhibitors ameliorate schizophrenia-associated dendritic spine deterioration in vitro and in vivo during late adolescence. *Proceedings of the National Academy of Sciences*, *111*(17), 6461-6466.

Hering, H., & Sheng, M. (2001). Dentritic spines: structure, dynamics and regulation. *Nature Reviews Neuroscience*, *2*(12), 880-888.

Hofer, S. B., Mrsic-Flogel, T. D., Bonhoeffer, T., & Hübener, M. (2009). Experience leaves a lasting structural trace in cortical circuits. *Nature*, *457*(7227), 313-317.

Honea, R. A., Meyer-Lindenberg, A., Hobbs, K. B., Pezawas, L., Mattay, V. S., Egan, M. F., Verchinski, B., Passingham, R. E., Weinberger, D. R., & Callicott, J. H. (2008). Is gray matter volume an intermediate phenotype for schizophrenia? A voxel-based morphometry study of patients with schizophrenia and their healthy siblings. *Biological psychiatry*, *63*(5), 465-474.

Honkura, N., Matsuzaki, M., Noguchi, J., Ellis-Davies, G. C., & Kasai, H. (2008). The subspine organization of actin fibers regulates the structure and plasticity of dendritic spines. *Neuron*, *57*(5), 719-729.

Huh, G. S., Boulanger, L. M., Du, H., Riquelme, P. A., Brotz, T. M., & Shatz, C. J. (2000). Functional requirement for class I MHC in CNS development and plasticity. *Science*, *290*(5499), 2155-2159.

Iwata, Y., Nakajima, S., Suzuki, T., Keefe, R. S. E., Plitman, E., Chung, J. K., Caravaggio, F., Mimura, M., Graff-Guerrero, A., & Uchida, H. (2015). Effects of glutamate positive modulators on cognitive deficits in schizophrenia: a systematic review and meta-analysis of double-blind randomized controlled trials. *Molecular psychiatry*, *20*(10), 1151-1160.

Jones, C. A., Watson, D. J. G., & Fone, K. C. F. (2011). Animal models of schizophrenia. *British journal of pharmacology*, *164*(4), 1162-1194.

Kang, H. J., Voleti, B., Hajszan, T., Rajkowska, G., Stockmeier, C. A., Licznerski, P., Lepack, A., Majik, M. S., Jeong, L. K., Banasr, M., Son, H., & Duman, R. S. (2012). Decreased expression of synapse-related genes and loss of synapses in major depressive disorder. *Nature medicine*, *18*(9), 1413-1417.

Kang, J., Park, H., & Kim, E. (2016). IRSp53/BAIAP2 in dendritic spine development, NMDA receptor regulation, and psychiatric disorders. *Neuropharmacology*, *100*, 27-39.

Kantrowitz, J. T., Woods, S. W., Petkova, E., Cornblatt, B., Corcoran, C. M., Chen, H., Silipo, G., & Javitt, D. C. (2015). D-serine for the treatment of negative symptoms in individuals at clinical high risk of schizophrenia: a pilot, double-blind, placebo-controlled, randomised parallel group mechanistic proof-of-concept trial. *The Lancet Psychiatry*, *2*(5), 403-412.

Kassem, M. S., Lagopoulos, J., Stait-Gardner, T., Price, W. S., Chohan, T. W., Arnold, J. C., Hatton, S. N., & Bennett, M. R. (2013). Stress-induced grey matter loss determined by MRI is primarily due to loss of dendrites and their synapses. *Molecular neurobiology*, *47*(2), 645-661.

Kim, I. H., Racz, B., Wang, H., Burianek, L., Weinberg, R., Yasuda, R., Wetsel, W. C., & Soderling, S. H. (2013). Disruption of Arp2/3 results in asymmetric structural plasticity of dendritic spines and progressive synaptic and behavioral abnormalities. *Journal of Neuroscience*, *33*(14), 6081-6092.

Kim, M. H., Choi, J., Yang, J., Chung, W., Kim, J. H., Paik, S. K., Kim, K., Han, S., Won, H., Bae, Y., Cho, S., Seo, J., Bae, Y. C., Choi, S., & Kim, E. (2009). Enhanced NMDA receptor-mediated synaptic transmission, enhanced long-term potentiation, and impaired learning and memory in mice lacking IRSp53. *Journal of Neuroscience*, *29*(5), 1586-1595.

Kolomeets, N. S., Orlovskaya, D. D., Rachmanova, V. I., & Uranova, N. A. (2005). Ultrastructural alterations in hippocampal mossy fiber synapses in schizophrenia: a postmortem morphometric study. *Synapse*, *57*(1), 47-55.

Konopaske, G. T., Lange, N., Coyle, J. T., & Benes, F. M. (2014). Prefrontal cortical dendritic spine pathology in schizophrenia and bipolar disorder. *JAMA psychiatry*, *71*(12), 1323-1331.

Koren, D., Seidman, L. J., Harrison, R. H., Lyons, M. J., Kremem, W. S., Caplan, B., Goldstein, J. M., Faraone, S. V., & Tsuang, M. T. (1998). Factor structure of the Wisconsin Card Sorting Test: dimensions of deficit in schizophrenia. *Neuropsychology*, *12*(2), 289.

Korobova, F., & Svitkina, T. (2010). Molecular architecture of synaptic actin cytoskeleton in hippocampal neurons reveals a mechanism of dendritic spine morphogenesis. *Molecular biology of the cell*, *21*(1), 165-176.

Lai, C. S. W., Adler, A., & Gan, W. B. (2018). Fear extinction reverses dendritic spine formation induced by fear conditioning in the mouse auditory cortex. *Proceedings of the National Academy of Sciences*, *115*(37), 9306-9311.

Lazar, N. L., Rajakumar, N., & Cain, D. P. (2008). Injections of NGF into neonatal frontal cortex decrease social interaction as adults: a rat model of schizophrenia. *Schizophrenia bulletin*, *34*(1), 127-136.

Lee, F. H., Fadel, M. P., Preston-Maher, K., Cordes, S. P., Clapcote, S. J., Price, D. J., Roder., J. C., & Wong, A. H. (2011). Disc1 point mutations in mice affect development of the cerebral cortex. *Journal of Neuroscience*, *31*(9), 3197-3206.

Leuner, B., & Gould, E. (2010). Dendritic growth in medial prefrontal cortex and cognitive flexibility are enhanced during the postpartum period. *Journal of Neuroscience*, *30*(40), 13499-13503.

Li, C. S. R. (2004). Do schizophrenia patients make more perseverative than non-perseverative errors on the Wisconsin Card Sorting Test? A meta-analytic study. *Psychiatry research*, *129*(2), 179-190.

Li, L., Deng, B., Li, S., Liu, Z., Jiang, T., Xiao, Z., & Wang, Q. (2017). TAT-PEP, a novel blocker of PirB, enhances the recovery of cognitive function in mice after transient global cerebral ischemia. Behavioural brain research, 326, 322-330.

Li, N., Lee, B., Liu, R. J., Banasr, M., Dwyer, J. M., Iwata, M., Li, X., Aghajanian, G., & Duman, R. S. (2010). mTOR-dependent synapse formation underlies the rapid antidepressant effects of NMDA antagonists. *Science*, *329*(5994), 959-964.

McGuier, N. S., Uys, J. D., & Mulholland, P. J. (2019). Neural morphology and addiction. In *Neural Mechanisms of Addiction* (pp. 123-135). Academic Press.

McNeill, T. H., Brown, S. A., Rafols, J. A., & Shoulson, I. (1988). Atrophy of medium spiny I striatal dendrites in advanced Parkinson's disease. *Brain research*, *455*(1), 148-152.

Merino-Serrais, P., Benavides-Piccione, R., Blazquez-Llorca, L., Kastanauskaite, A., Rabano, A., Avila, J., & DeFelipe, J. (2013). The influence of phospho-tau on dendritic spines of cortical pyramidal neurons in patients with Alzheimer's disease. *Brain*, *136*(6), 1913-1928.

Mi, Y. J., Chen, H., Guo, N., Sun, M. Y., Zhao, Z. H., Gao, X. C., Wang, X. L., Zhang, R. S., Zhou, J. B., & Gou, X. C. (2017). Inhibition of PirB activity by TAT-PEP improves mouse motor ability and cognitive behavior. *Frontiers in aging neuroscience*, *9*, 199.

Milner, B. (1963). Effects of different brain lesions on card sorting: The role of the frontal lobes. *Archives of neurology*, *9*(1), 90-100.

Mirnics, K., Middleton, F. A., Stanwood, G. D., Lewis, D. A., & Levitt, P. (2001). Disease-specific changes in regulator of G-protein signaling 4 (RGS4) expression in schizophrenia. *Molecular psychiatry*, *6*(3), 293-301.

Moczulska, K. E., Tinter-Thiede, J., Peter, M., Ushakova, L., Wernle, T., Bathellier, B., & Rumpel, S. (2013). Dynamics of dendritic spines in the mouse auditory cortex during memory formation and memory recall. *Proceedings of the National Academy of Sciences*, *110*(45), 18315-18320.

Murmu, M. S., Salomon, S., Biala, Y., Weinstock, M., Braun, K., & Bock, J. (2006). Changes of spine density and dendritic complexity in the prefrontal cortex in offspring of mothers exposed to stress during pregnancy. *European Journal of Neuroscience*, *24*(5), 1477-1487.

Nelson, H. E. (1976). A modified card sorting test sensitive to frontal lobe defects. *Cortex*, *12*(4), 313-324.

Ostroff, L. E., Fiala, J. C., Allwardt, B., & Harris, K. M. (2002). Polyribosomes redistribute from dendritic shafts into spines with enlarged synapses during LTP in developing rat hippocampal slices. *Neuron*, *35*(3), 535-545.

Papadopoulos, C. M., Tsai, S. Y., Cheatwood, J. L., Bollnow, M. R., Kolb, B. E., Schwab, M. E., & Kartje, G. L. (2006). Dendritic plasticity in the adult rat following middle cerebral artery occlusion and Nogo-a neutralization. *Cerebral Cortex*, *16*(4), 529-536.

Park, M., Salgado, J. M., Ostroff, L., Helton, T. D., Robinson, C. G., Harris, K. M., & Ehlers, M. D. (2006). Plasticity-induced growth of dendritic spines by exocytic trafficking from recycling endosomes. *Neuron*, *52*(5), 817-830.

Paxinos, G., & Watson, C. (2006). *The rat brain in stereotaxic coordinates: hard cover edition*. Elsevier.

Peters, A., Sethares, C., & Luebke, J. I. (2008). Synapses are lost during aging in the primate prefrontal cortex. *Neuroscience*, *152*(4), 970-981.

Peters, A., & Kaiserman-Abramof, I. R. (1970). The small pyramidal neuron of the rat cerebral cortex. The perikaryon, dendrites and spines. *American Journal of Anatomy*, *127*(4), 321-355.

Placek, K., Dippel, W. C., Jones, S., & Brady, A. M. (2013). Impairments in set-shifting but not reversal learning in the neonatal ventral hippocampal lesion model of schizophrenia: further evidence for medial prefrontal deficits. *Behavioural brain research*, *256*, 405-413.

Radley, J. J., Rocher, A. B., Miller, M., Janssen, W. G., Liston, C., Hof, P. R., McEwen, B. S., & Morrison, J. H. (2006). Repeated stress induces dendritic spine loss in the rat medial prefrontal cortex. *Cerebral cortex*, *16*(3), 313-320.

Rajakumar, N., Leung, L. S., Ma, J., Rajakumar, B., & Rushlow, W. (2004). Altered neurotrophin receptor function in the developing prefrontal cortex leads to adult-onset dopaminergic hyperresponsivity and impaired prepulse inhibition of acoustic startle. *Biological psychiatry*, *55*(8), 797-803.

Rajakumar, R., & Rajakumar, B. (2005). A mild disruption of subplate function in the developing prefrontal cortex is sufficient to cause multiple neuropathological features of schizophrenia. *Schizophrenia Bulletin*, *31*(2), 308-309.

Roberts, R. C., Conley, R., Kung, L., Peretti, F. J., & Chute, D. J. (1996). Reduced striatal spine size in schizophrenia: a postmortem ultrastructural study. *Neuroreport*, *7*(6), 1214-1218.

Rüsch, N., Spoletini, I., Wilke, M., Bria, P., Di Paola, M., Di Iulio, F., Martinotti, G., Caltagirone, C., & Spalletta, G. (2007). Prefrontal–thalamic–cerebellar gray matter networks and executive functioning in schizophrenia. *Schizophrenia Research*, *93*(1-3), 79-89.

Sala, C., & Segal, M. (2014). Dendritic spines: the locus of structural and functional plasticity. *Physiological reviews*, *94*(1), 141-188.

Satoh, A., Nakanishi, H., Obaishi, H., Wada, M., Takahashi, K., & Satoh, K. (1998). An actin filament-binding protein with one Pdz domain localized at cadherin-based cell-cell adhesion sites. *J Biol Chem*, *273*, 3470-3475.

Sawallisch, C., Berhörster, K., Disanza, A., Mantoani, S., Kintscher, M., Stoenica, L., Dityatev, A., Sieber, S., Kindler, S., Morellini, F., Schweizer, M., Boeckers, T. M., Korte, M., Scita, G., & Kreienkamp, H. J. (2009). The insulin receptor substrate of 53 kDa (IRSp53) limits hippocampal synaptic plasticity. *Journal of Biological Chemistry*, *284*(14), 9225-9236.

Scita, G., Confalonieri, S., Lappalainen, P., & Suetsugu, S. (2008). IRSp53: crossing the road of membrane and actin dynamics in the formation of membrane protrusions. *Trends in cell biology*, *18*(2), 52-60.

Scheff, S. W., Price, D. A., Schmitt, F. A., & Mufson, E. J. (2006). Hippocampal synaptic loss in early Alzheimer's disease and mild cognitive impairment. *Neurobiology of aging*, *27*(10), 1372-1384.

Sheu, J. R., Hsieh, C. Y., Jayakumar, T., Tseng, M. F., Lee, H. N., Huang, S. W., Manubolu, M., & Yang, C. H. (2019). A critical period for the development of schizophrenia-like pathology by aberrant postnatal neurogenesis. *Frontiers in neuroscience*, *13*, 635.

Soetanto, A., Wilson, R. S., Talbot, K., Un, A., Schneider, J. A., Sobiesk, M., Kelly, J., Leurgans, S., Bennett, D. A., & Arnold, S. E. (2010). Association of anxiety and depression with microtubule-associated protein 2–and synaptopodin-immunolabeled dendrite and spine densities in hippocampal CA3 of older humans. *Archives of general psychiatry*, *67*(5), 448-457.

Steen, E., Terry, B. M., J Rivera, E., Cannon, J. L., Neely, T. R., Tavares, R., Xu, J. X., Wands, J. R., & de la Monte, S. M. (2005). Impaired insulin and insulin-like growth factor expression and signaling mechanisms in Alzheimer's disease–is this type 3 diabetes?. *Journal of Alzheimer's disease*, *7*(1), 63-80.

Stephens, B., Mueller, A. J., Shering, A. F., Hood, S. H., Taggart, P., Arbuthnott, G. W., Bell, J. E., Kilford, L., Kingsbury, A. E., Daniel, S. E., & Ingham, C. A. (2005). Evidence of a breakdown of corticostriatal connections in Parkinson's disease. *Neuroscience*, *132*(3), 741-754.

Streit, J., Spenger, C., & Lüscher, H. R. (1991). An organotypic spinal cord-dorsal root ganglion-skeletal muscle coculture of embryonic rat. II. Functional evidence for the formation of spinal reflex arcs in vitro. *European Journal of Neuroscience*, *3*(11), 1054-1068.

Sweet, R. A., Henteleff, R. A., Zhang, W., Sampson, A. R., & Lewis, D. A. (2009). Reduced dendritic spine density in auditory cortex of subjects with schizophrenia. *Neuropsychopharmacology*, *34*(2), 374-389.

Syken, J., GrandPre, T., Kanold, P. O., & Shatz, C. J. (2006). PirB restricts ocular-dominance plasticity in visual cortex. *Science*, *313*(5794), 1795-1800.

Takai, T. (2005). Paired immunoglobulin-like receptors and their MHC class I recognition. *Immunology*, *115*(4), 433-440.

Talpos, J. C. (2017). Symptomatic thinking: the current state of Phase III and IV clinical trials for cognition in schizophrenia. *Drug discovery today*, *22*(7), 1017-1026.

Terry, R. D., Masliah, E., Salmon, D. P., Butters, N., DeTeresa, R., Hill, R., Hansen, L. A., & Katzman, R. (1991). Physical basis of cognitive alterations in Alzheimer's disease: synapse loss is the major correlate of cognitive impairment. *Annals of Neurology: Official Journal of the American Neurological Association and the Child Neurology Society*, *30*(4), 572-580.

Tropea, D., Sur, M., & Majewska, A. K. (2011). Experience-dependent plasticity in visual cortex: Dendritic spines and visual responsiveness. *Communicative & integrative biology*, *4*(2), 216-219.

Van Harreveld, A., & Fifkova, E. (1975). Swelling of dendritic spines in the fascia dentata after stimulation of the perforant fibers as a mechanism of post-tetanic potentiation. *Experimental neurology*, *49*(3), 736-749.

Vidal, G. S., Djurisic, M., Brown, K., Sapp, R. W., & Shatz, C. J. (2016). Cell-autonomous regulation of dendritic spine density by PirB. *Eneuro*, *3*(5).

Villalba, R. M., Lee, H., & Smith, Y. (2009). Dopaminergic denervation and spine loss in the striatum of MPTP-treated monkeys. *Experimental neurology*, *215*(2), 220-227.

Watson, G. S., Cholerton, B. A., Reger, M. A., Baker, L. D., Plymate, S. R., Asthana, S., Fishel, M. A., Kulstad, J. J., Green, P. S., Cook, D. G., Kahn, S. E., Keeling, M. L., & Craft, S. (2005). Preserved cognition in patients with early Alzheimer disease and amnestic mild cognitive impairment during treatment with rosiglitazone: a preliminary study. *The American journal of geriatric psychiatry*, *13*(11), 950-958.

Wieczerzak, K. B., Patel, S. V., MacNeil, H., Scott, K. E., Schormans, A. L., Hayes, S. H., Herrmann, B., & Allman, B. L. (2021). Differential Plasticity in Auditory and Prefrontal Cortices, and Cognitive-Behavioral Deficits Following Noise-Induced Hearing Loss. *Neuroscience*, *455*, 1-18.

Yang, X. D., Liao, X. M., Uribe-Marino, A., Liu, R., Xie, X. M., Jia, J., Su, Y. A., Li, J. T., Schmidt, M. V., Wang, X. D., & Si, T. M. (2015). Stress during a critical postnatal period induces region-specific structural abnormalities and dysfunction of the prefrontal cortex via CRF 1. *Neuropsychopharmacology*, *40*(5), 1203-1215.

Yi, Z., Fan, X., Wang, J., Liu, D., Freudenreich, O., Goff, D., & Henderson, D. C. (2012). Rosiglitazone and cognitive function in clozapine-treated patients with schizophrenia: a pilot study. *Psychiatry research*, *200*(2-3), 79-82.

Young, M. E., Ohm, D. T., Dumitriu, D., Rapp, P. R., & Morrison, J. H. (2014). Differential effects of aging on dendritic spines in visual cortex and prefrontal cortex of the rhesus monkey. *Neuroscience*, *274*, 33-43.

Zaja-Milatovic, S., Milatovic, D., Schantz, A. M., Zhang, J., Montine, K. S., Samii, A., Deutch, A. Y., & Montine, T. J. (2005). Dendritic degeneration in neostriatal medium spiny neurons in Parkinson disease. *Neurology*, *64*(3), 545-547.

Zaqout, S., & Kaindl, A. M. (2016). Golgi-Cox staining step by step. *Frontiers in neuroanatomy*, *10*, 38.

Zarate Jr, C. A., Singh, J. B., Quiroz, J. A., De Jesus, G., Denicoff, K. K., Luckenbaugh, D. A., Manji, H. K., & Charney, D. S. (2006). A double-blind, placebo-controlled study of memantine in the treatment of major depression. *American Journal of Psychiatry*, *163*(1), 153-155.

Zhang, S., Boyd, J., Delaney, K., & Murphy, T. H. (2005). Rapid reversible changes in dendritic spine structure in vivo gated by the degree of ischemia. *Journal of Neuroscience, 25*(22), 5333-5338.

Appendices

Appendix A. The effects of noise exposure on stimulus-response habit learning, set-shifting and reversal learning. (B) Compared to the shams (grey; n = 11), the noise-exposed rats (blue; n = 11) committed significantly more errors during the visual-cue discrimination (VCD) task (*p < 0.001); findings consistent with impaired stimulus–response habit learning. **(C)** The noise-exposed rats also trended toward a greater number of errors during the VCD retrieval task performed 24 h later; however, these data did not reach statistical significance. **(D)** Immediately following the VCD retrieval trials, the task shifted to a response discrimination (RD), in which the rats had to learn that the side opposite to their side-bias (e.g. left) was now the correct response regardless of the cue light. **(E)** Noise exposure did not appear to affect the rats' ability to set-shift, as the shams and noise-exposed rats committed a similar number of errors during the RD task. **(F)** Similar to the VCD retrieval trials, there was a trend for the noise-exposed rats to perform more errors than the shams during the retrieval trials performed 24 h after the RD task, yet the results were not statistically significant. **(G)** Immediately following the RD retrieval trials, the rules of the task were reversed such that the rats had to learn to press the opposite lever (e.g., right). **(H)** During the reversed-RD task, the noise-exposed rats committed a similar number of errors as the shams; findings which suggest that the rats' reversal learning was not impaired following noise exposure. Data represent group mean ± SEM. (Image and caption adapted from Wieczerzak et al., 2021).
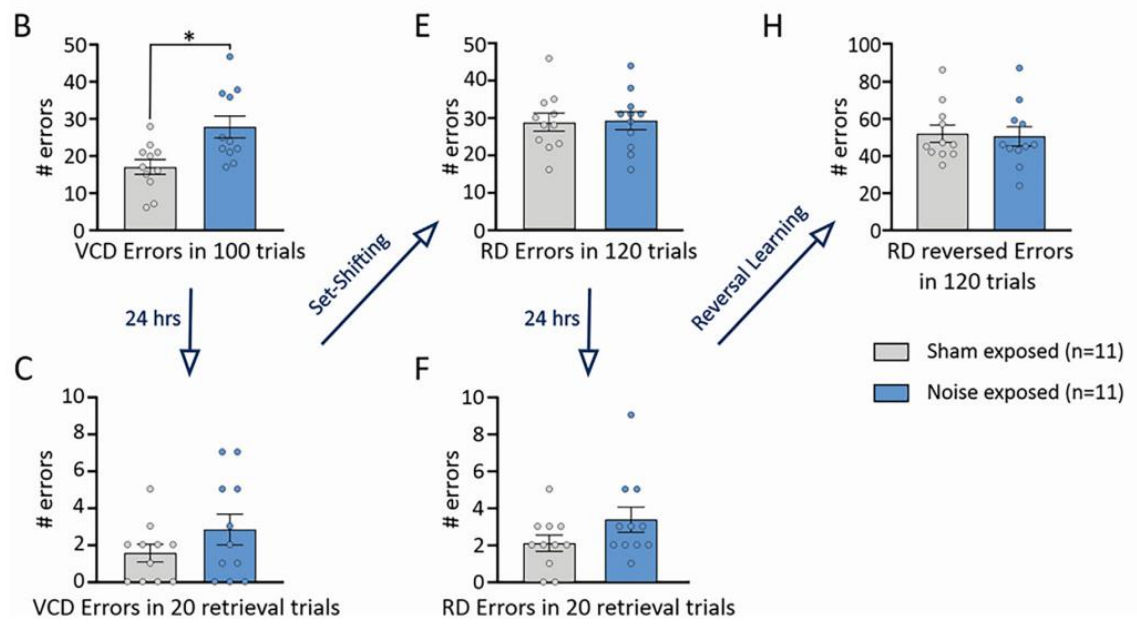
Curriculum Vitae

Name: Hannah Jaye MacNeil

Post-secondary Education and Degrees:

Dalhousie University
Halifax, Nova Scotia, Canada
Sept 2014 – June 2018
B.Sc. Honours, Neuroscience

University of Western Ontario
London, Ontario, Canada
Sept 2018 – June 2021
M.Sc. Neuroscience

Honours and Awards:

Natural Sciences and Engineering Research Council (NSERC)
Jan 2019 – Dec 2020

Dalhousie First Class Honours Distinction
Sept 2017 – June 2018

Brimer Memorial Scholarship
Sept 2017 – June 2018

NewPage Port Hawkesbury Scholarship
Sept 2017 – June 2018

Dalhousie University Dean's List
Sept 2015 – June 2018

Related Work Experience

Pre-Graduate Student Researcher
University of Western Ontario
June 2018 – Sept 2018

Undergraduate Student Summer Researcher
Dalhousie University
May 2017 – Sept 2017

Publications:

Wieczerzak, K. B., Patel, S. V., **MacNeil, H.,** Scott, K. E., Schormans, A. L., Hayes, S. H., Herrmann, B., & Allman, B. L. (2021). Differential Plasticity in Auditory and Prefrontal Cortices, and Cognitive-Behavioral Deficits Following Noise-Induced Hearing Loss. *Neuroscience*, *455*, 1-18.